MASTER THESIS

Technical Medicine

Towards the application of virtual preoperative planning and patient specific guides in complex foot surgery

Elske Bergwerff

7 december 2021

EXAMINATION COMMITTEE

Prof. Dr. Ir. G.J. Verkerke[1]	Chairman
Dr. A.V.C.M. Zeegers[2]	Medical supervisor
Ir. E.E.G. Hekman[1]	Technical supervisor
Drs. R.M. Krol[3]	Process supervisor
Dr. F.J. Siepel[3]	External member
Dr. M.A. Koenrades[4]	Additional member

1. Faculty of engineering technology, University of Twente

2. Department of orthopaedics, Medisch Spectrum Twente

3. TechMed Centre, University of Twente

4. 3D lab, Medisch Spectrum Twente

Medisch Spectrum Twente
een santeon ziekenhuis

UNIVERSITY OF TWENTE.

Table of contents

Abstract

Complex foot deformity is a multiplanar deformity of the foot, for which surgical correction is necessary. Preoperative planning of complex foot surgery at Medisch Spectrum Twente (MST) is currently based on reference angles describing healthy foot anatomy in combination with a 3D printed model of the foot, obtained from CT data. The digital 3D model may further be used to virtually plan corrective surgery and design patient specific guides (PSGs). The aim of this study was to determine how virtual planning and PSGs can be applied in complex foot surgery at MST. We have developed workflows for acquisition of an accurate foot model, virtual planning of complex foot surgery and PSG design.

An accurate foot model is an anatomically correct foot model, which enables the use of non-weightbearing reference angles during virtual planning. The effect of manual redressing of the foot was studied in two cases of rigid foot deformity to determine how the foot should be positioned during CT acquisition. The results show that the natural supine alignment differs from the maximum achievable neutral alignment. Therefore, CT data should be acquired with the foot set in the neutral alignment.

The effect of virtual planning was studied by comparing two cases: one treated with, and one treated without virtual planning. The within-subject change in foot anatomy was compared between these cases based on measured reference angles. Additionally, the measured reference angles in the preoperative foot, postoperative foot and planned result were all compared to normal values. The results indicate an improved postoperative foot alignment when applying virtual planning in comparison to the current treatment.

Initial PSG designs were developed and tested *in vitro* in consultation with one orthopaedic surgeon. The final design consisted of a proximal cutting/repositioning guide in combination with a distal repositioning guide. The design for the cutting/repositioning guide was promising, but adaptations to the repositioning guide are needed before application during surgery is possible.

In summary, we found that CT data should be acquired from a neutrally positioned foot to enable the use of normal values for reference angles during virtual planning. The cases studied in this thesis demonstrate that the application of virtual planning in complex foot surgery can already result in a more optimal postoperative foot alignment compared to the current treatment. The application of PSGs may improve the result of complex foot surgery even further, but the current PSG design must be improved and validated before it can be applied in complex foot surgery.

List of abbreviations

2D	-	Two-dimensional
3D	-	Three-dimensional
CAD-software	-	Computer Aided Design software
CIA	-	Calcaneal inclination angle
CM2	-	Calcaneal-second metatarsal angle
CM3	-	Calcaneal-third metatarsal angle
CM5	-	Calcaneal-fifth metatarsal angle
CROW	-	Charcot Restrain Orthotic Walker
CT	-	Computed Tomography
DA	-	Djian-Annonier Angle
DP	-	Dorsoplantar
K-wire	-	Kirschner wire
MPR	-	Multiplanar reconstructed
MST	-	Medisch Spectrum Twente
Osteotomy	-	Bone cut
PSG	-	Patient Specific Guide
TCA	-	Talocalcaneal angle

Chapter 1 – Introduction

Anatomy of the foot

The foot is a crucial part of the musculoskeletal system, being the weightbearing part of the human body. The foot is important in stabilizing the body during the complete gait cycle and crucial for push-off during walking. The foot consists of 26 bones aligned by joints and ligaments in a plantigrade orientation, which can be seen in Figure 1.1. The osseous anatomy of the foot can be divided into three parts: the hindfoot, midfoot and forefoot. The hindfoot consists of the Calcaneus and the Talus, of which the latter is the only bone in the foot conjoined with the lower leg. Due to the special configuration of the Talus, movement of the foot is possible in all three planes. The midfoot consists of the Navicular, Cuboid and three Cuneiform bones (medial, intermediate and lateral). The forefoot consists of the metatarsals and phalanges, which are anatomically numbered medial to lateral, and all consist of a proximal base, shaft and distal head. The first digit has a proximal and distal phalanx, the other four digits have an additional middle phalanx. Plantar to the first metatarsal head lie two sesamoid bones (medial and lateral). Weightbearing areas are found on the sole of the foot at the tuberosity of the calcaneus, the sesamoid bones of the first metatarsal and the fifth metatarsal head. (1,2)

Complex foot deformities

Foot deformity is a malalignment of the bones in the foot. Three of the most common types of foot deformity are pes cavus, pes planus and pes equino varus (clubfoot). (3) Pes cavus, also known as a hollow foot, is characterized by a heightened arch and is mainly caused by a neuromuscular disease, trauma, the presence of a residual clubfoot or idiopathic causes. (4) Pes planus, also known as flat foot, is characterized by a fallen arch and is either congenital or acquired by posterior tibial tendon dysfunction, trauma, diabetes mellitus, congenital disease or arthropathy. (5)

Complex foot deformity is a multiplanar, angular, rotational and translational deformity of the foot, often progressing in severity over time. An example of complex foot deformity is Charcot foot. Charcot

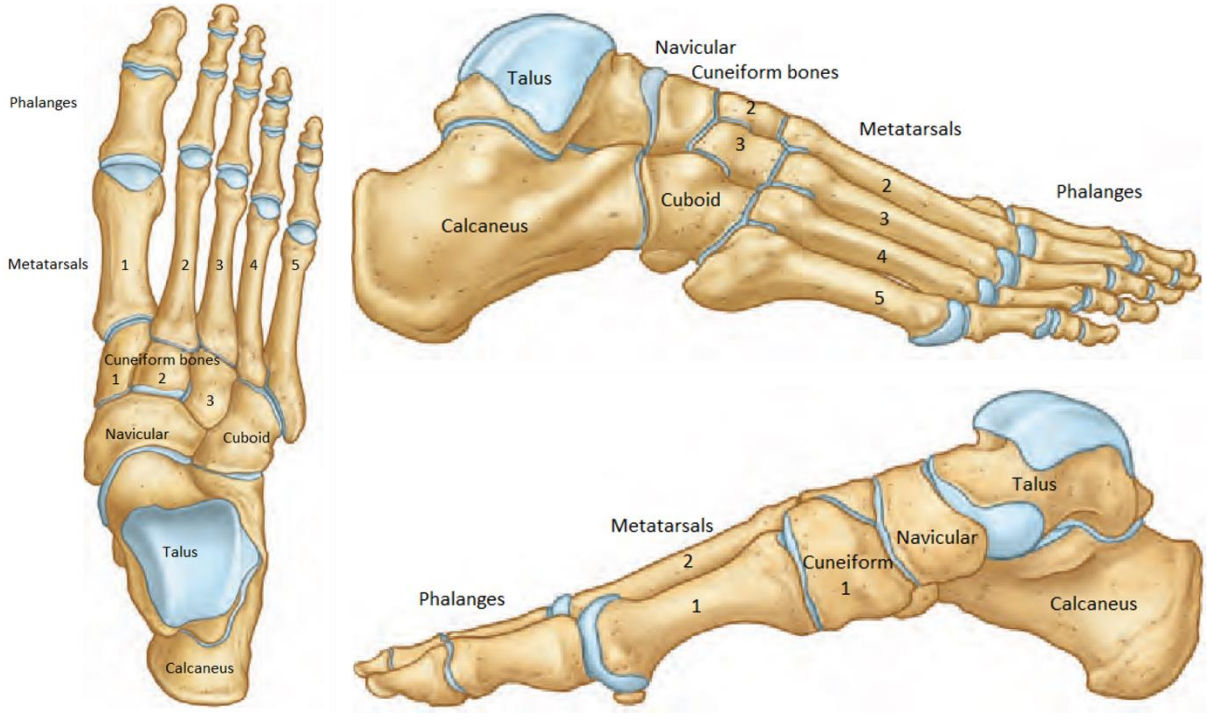

Figure 1.1: The osseous anatomy of the plantigrade oriented foot in superior (left), lateral (top-right) and medial (bottom-right) view, adaptation from (1)

foot is caused by (diabetic) polyneuropathy leading to sensory loss in the foot. A minor incident like a sprain or microfracture does not result in pain-sensation in a diabetic foot. The patient will continue weightbearing, which in case of microfracture or ligament injuries leads to initial bone deformity, subluxation or dislocation. When the deformity is not treated and weightbearing continues, the foot deformity progresses into a complex foot deformity, with possible pressure ulcerations and wounds. In severe cases, the complex foot deformity is even combined with osteomyelitis. (6)

The diagnostic process when a patient presents with symptoms indicating foot deformity consists of consultation, physical examination and radiographic examination of the foot. Static two-dimensional (2D) weightbearing lateral and dorsoplantar (DP) radiographs are obtained to assess the foot anatomy and alignment for underlying causes of the symptoms. Additional axial images are obtained when assessment of the ankle is necessary. (7,8) Acquisition of 2D radiographs follows a standard protocol consisting of foot positioning during image acquisition and distance and angulation between foot and X-ray source to ensure a correct projection plane. (7)

Assessment of foot anatomy in 2D radiographs is based on comparison of measured reference angles to normal values describing healthy foot anatomy and alignment. These reference angles contain information about the alignment of the fore-, mid- and hindfoot itself and their alignment relative to each other in the two-dimensional space. The reference angles are measured between the longitudinal axes of specific bones and compared to the normal values found in literature. (7–9)

Reference angles have been determined by many different researchers. Lamm et al. (7) and Carrara et al. (8) both conducted a literature review to provide a clear overview of the most common reference angles including definitions and schematic representations of these angles. Lamm et al. also included normal values of the recorded reference angles based on measurements in weightbearing radiographs of 24 healthy feet. (7) Appendix A contains an overview of reference angles mentioned in these two articles, including schematics for determination of the reference lines used in measurement of the reference angles.

Current treatment of complex foot deformities

Treatment options for foot deformity differ with severity. In mild cases, regular surveillance in combination with immobilization is applied to prevent weight bearing and thereby progression of the deformity. In complex cases, consisting of multiple rotational and translational deformities and where conservative treatment does not suffice, surgical correction is necessary. Main indications for corrective surgery are severe deformities and instability of the foot which might lead to limb-threatening ulcerations and osteomyelitis, provided that vascularisation in the lower leg and foot is sufficient. (6,10,11) The goals of surgical treatment are to restore the foot into a plantigrade orientation, restore balance to the foot, minimize chance of ulceration and enable mobility by means of (bespoke) footwear. (11,12)

Surgical corrections of complex foot deformities are generally planned using the reference angles determined in 2D weightbearing radiographs. (7,8,13) Restoration of these angles ensures a good lower limb function and is, therefore, the basis of foot correction. (9) The bone cuts (osteotomies) needed to restore these angles into normal value range can be apprehended preoperatively using the radiographs. Execution of the correction, however, is based mainly on the surgeons' experience as surgical navigation and the application of surgical guides is difficult for the complex multiplanar deformity. (13–15)

Currently, at Medisch Spectrum Twente (MST) a three-dimensional (3D) model of the osseous anatomy is obtained from CT data and 3D printed in addition to the 2D radiographs for planning complex foot

surgery. This 3D printed anatomic model helps the surgeon in understanding the deformed anatomy and can be used to execute the procedure *in vitro* prior to surgery. The digital 3D model may further be used to virtually plan the corrective surgery and design patient specific guides (PSGs) using computer aided design software (CAD-software). (15–17) Virtual planning itself may already improve surgical outcome, as the 3D representation of CT data increases understanding of the deformity and necessary corrections. In addition, the use of a PSG can allow to perform the planned osteotomies more efficiently and accurately and achieve the planned correction. (15)

The application of virtual planning and PSGs is already increasing in the orthopaedic department for other osseous deformities, but is not commonly applied in complex foot surgery yet. (16,18,19) These surgeries could, however, benefit from the use of PSGs to improve surgical outcome, decrease surgical duration and decrease dependency on the surgeons' expertise. In an earlier study, Dagneaux et al. showed that it is possible to perform osteotomies using a PSG in one midfoot tarsectomy surgery. (14) Building on this study, Sobrón et al. applied PSGs successfully in three cavus midfoot corrections. (20) Further prospective research is suggested by both research groups to evaluate and validate the use of virtual planning and PSGs before standard application in the treatment of complex foot deformity. (14,20)

Aim of this study

The aim of this study was to determine how virtual planning and PSGs can be applied safely and effectively in complex foot surgery at MST. The research question posed in this thesis is: *How can virtual planning and patient specific guides be applied in and improve the outcome of corrective surgery for complex foot deformity?*

Thesis outline

In this thesis, workflows are set up for application of virtual planning and PSG design for midfoot correction in complex foot deformities. These workflows are applied in and evaluated for four clinical cases of complex foot deformity. In the second chapter, a description is given of the four cases used in one or more of the following chapters. This description contains information about the pathology and treatment(plan) including preoperative and – if available – postoperative imaging.

In the third chapter, a workflow for acquiring a virtual 3D model of the affected foot was developed. A case study was executed comparing foot alignment between supine and neutrally aligned feet using CT data of two patients to determine foot positioning during image acquisition.

In the fourth chapter, the constructed 3D model was used to develop a workflow for virtual planning of complex foot surgery. This workflow is applied in two clinical cases to study if applying virtual planning in complex foot surgery without the additional use of a patient specific guide can improve the surgical outcome. Evaluation was executed by comparing foot anatomy between planned results and postoperative results based on measured reference angles.

In the fifth chapter, the outcome of virtual planning of three clinical cases was used to develop a workflow for guide design for complex foot surgery. PSG design guidelines were formed based on defined prerequisites for structural and functional criteria. Based on these guidelines initial prototypes were developed and evaluated by one orthopaedic surgeon.

To conclude this thesis, the sixth chapter provides a general discussion, future perspectives and an overall conclusion.

Chapter 2 – Case description

Four patients were included in one or more of the case studies described in this thesis. In this chapter, a general description of each of these cases is given including imaging data. The numbering of these cases is applied in each of the following chapters.

Case A – Postoperative malposition

Patient description

A 30 year old female with spastic Cerebral Palsy causing complex foot deformity in the right foot. Triple arthrodesis executed in 2015 initially resulted in a correctly aligned foot with a fusion of the calcaneus, talus, navicular and cuboid bones. Over time, however, spasms in the posterior tibial tendon led to postoperative foot deformity consisting of malposition in varus supination and adduction with clawing of all toes.

Treatment plan

Correction of the postoperative foot deformity was executed five years after the initial triple arthrodesis. Preoperative planning of surgical treatment was executed before inclusion in this study and followed the current clinical protocol without virtual planning. The goal of complex foot surgery was release of the posterior tibial tendon and correction of the varus supination and adduction of the forefoot by a closing wedge osteotomy. The clawing of the toes was not included in the surgical correction at the choice of the patient.

Medical imaging

Preoperative CT data was acquired from a supinely aligned foot. A virtual model was created out of CT data and 3D printed to aid the orthopaedic surgeon during preoperative planning. (Figure 2.1) Postoperative CT data was acquired at 2 months follow-up with the foot set in a neutral position using a total contact cast (Figure 2.2). Weightbearing radiographs were acquired at 5 months follow-up in lateral and DP view. (Figure 2.3)

Application in this thesis

Supine preoperative CT data and neutral postoperative CT data were both used in the case study described in chapter 4 regarding virtual planning in complex foot deformity.

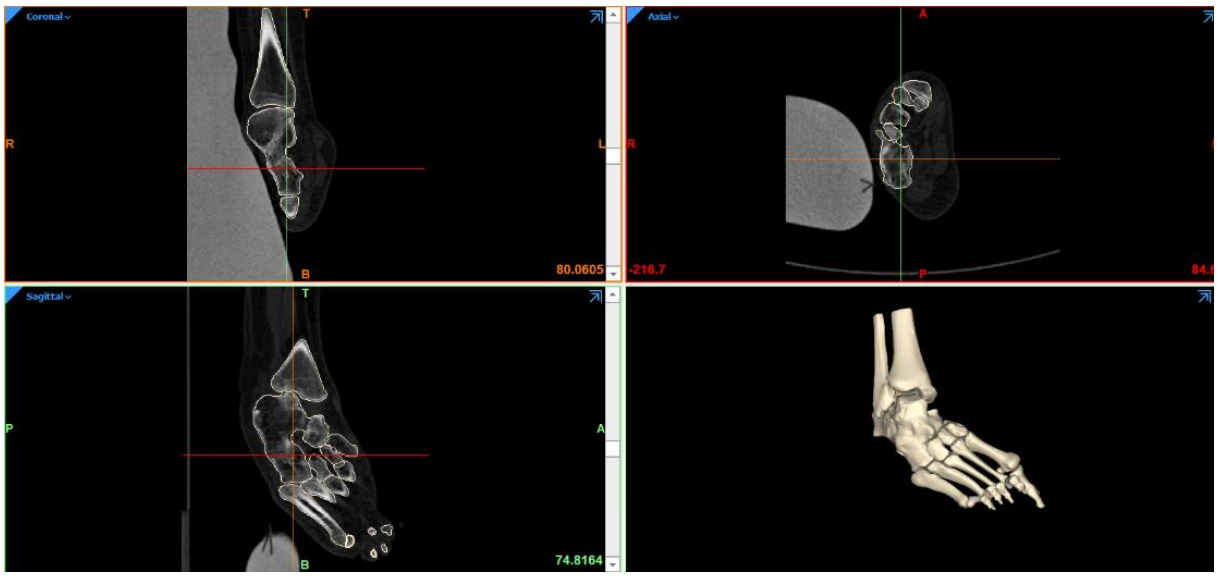

Figure 2.1: CT data of the supinely aligned preoperative foot of case A. Coronal (top left), Axial (top right) and Sagittal (bottom left) multiplanar reconstructed (MPR) views of CT data. The 3D model constructed from CT data is shown in the bottom right corner.

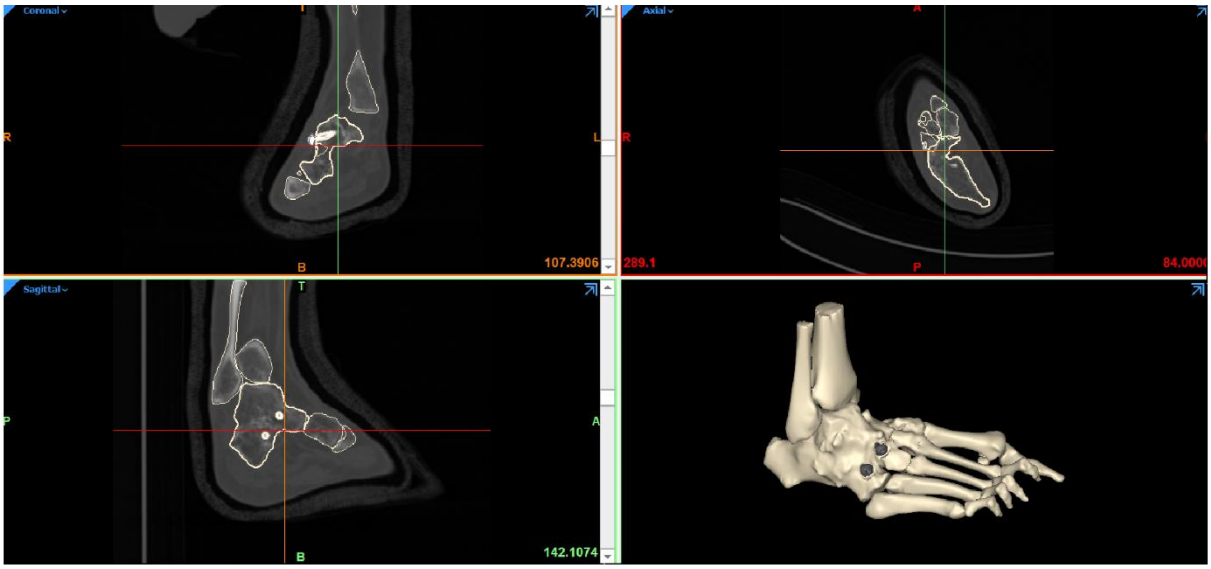

Figure 2.2: CT data of the postoperative foot of case A, acquired at 2 months follow-up with the foot set in a neutral alignment using a total contact cast. Coronal (top left), Axial (top right) and Sagittal (bottom left) MPR views of CT data. The 3D model constructed from CT data is shown in the bottom right corner.

Figure 2.3: Weightbearing radiographs in lateral (left) and DP (right) view of the postoperative foot of case A acquired at 5 months follow-up

Case B – Charcot foot

Patient description

A 55 year old male with Charcot foot resulting from diabetic polyneuropathy in the right foot, who already underwent correction of Charcot foot on the contralateral side following the current treatment protocol. Bilateral Charcot foot was diagnosed based on his medical history of Diabetes Mellitus, foot deformity with ulcerations, numbness in both feet and pain in every step. Progression of the deformity was prohibited preoperatively by foot redressing using a total contact cast. The complex foot deformity in the right foot consisted of dysplasia of the navicular, adduction and pronation of the forefoot and clawing of all toes.

Treatment plan

Surgical correction of the right foot was executed in two phases: forefoot reconstruction aiming to eliminate clawing of all toes without virtual planning according to the Jones procedure followed six weeks later by midfoot reconstruction with the addition of virtual planning. The aim of midfoot correction was to restore the longitudinal arch and restore the forefoot into a plantigrade orientation by execution of a closing wedge osteotomy.

Medical imaging

Preoperative CT data was acquired of both the supinely aligned foot and the neutrally aligned foot. Supine CT data was acquired before inclusion in this study and was acquired before forefoot reconstruction (Figure 2.4). As normal values for reference angle cannot be applied in virtual planning when using a supinely aligned foot, neutral CT data was acquired for virtual planning between forefoot and midfoot reconstruction (Figure 2.5). K-wires and screws placed during forefoot reconstruction were still in place during acquisition of neutral CT data causing distortion around the phalanges. Postoperative CT data was acquired at 4 months follow-up after the midfoot correction with the foot in a supine alignment. (Figure 2.6)

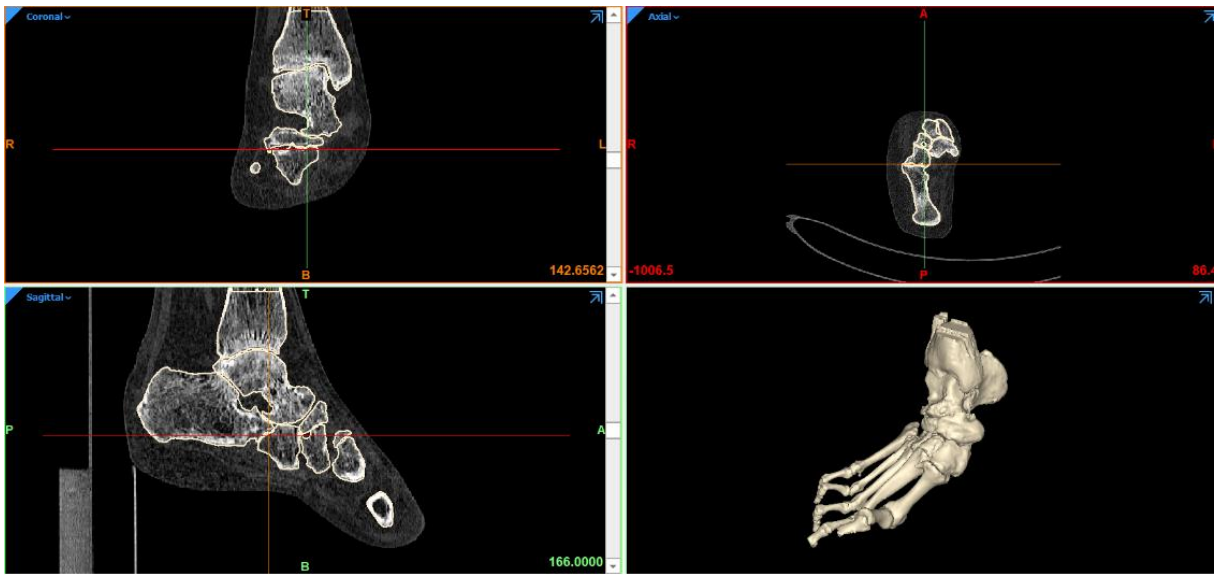

Figure 2.4: CT data of the supinely aligned preoperative foot of case B. Coronal (top left), Axial (top right) and Sagittal (bottom left) multiplanar reconstructed (MPR) views of CT data. The 3D model constructed from CT data is shown in the bottom right corner

Application in this thesis

Supine and neutral preoperative CT data were used in the case study described in chapter 3 regarding foot positioning during CT acquisition. Neutral preoperative CT data and supine postoperative CT data were both used in the case study described in chapter 4 regarding virtual planning in complex foot deformity. Neutral preoperative CT data was used in the case study described in chapter 5 regarding design of a patient specific guide.

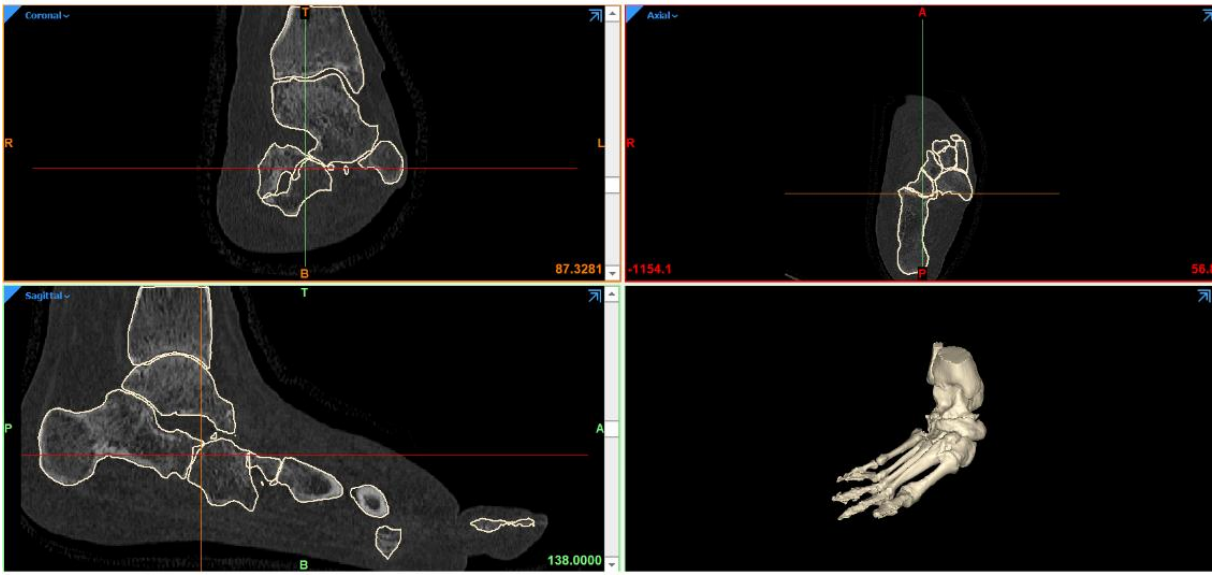

Figure 2.5: CT data of the preoperative foot of case B, neutrally aligned using a total contact cast. Distortion around phalanges is due to osteosynthesis material placed during forefoot reconstruction. Coronal (top left), Axial (top right) and Sagittal (bottom left) multiplanar reconstructed (MPR) views of CT data. The 3D model constructed from CT data is shown in the bottom right corner.

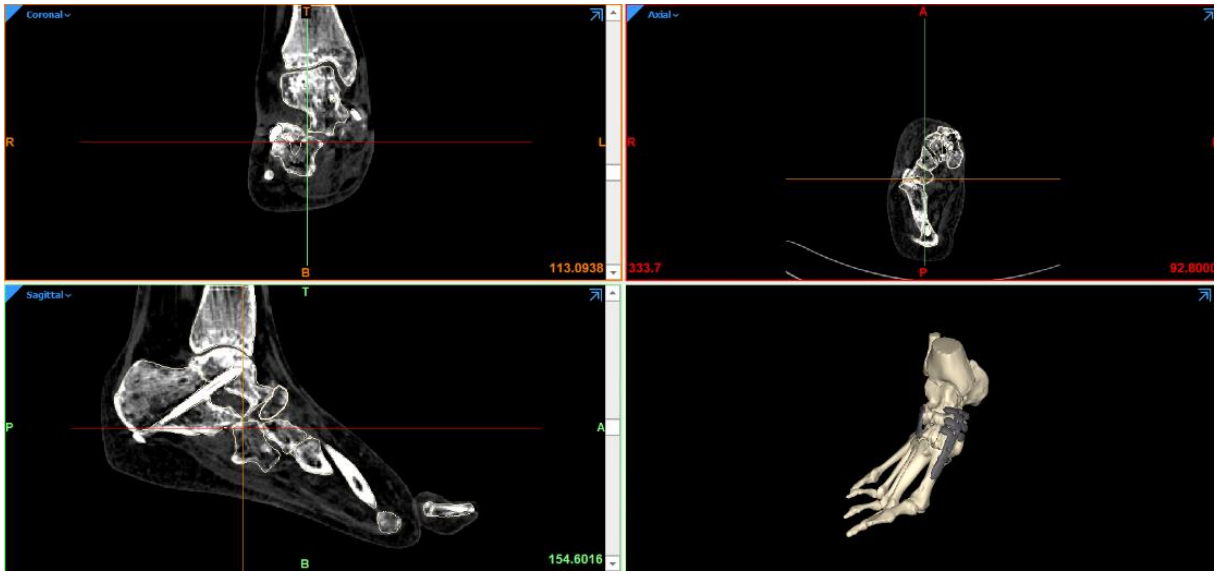

Figure 2.6: CT data of the supinely aligned postoperative foot of case B acquired at 4 months follow-up. Osteosynthesis material used in midfoot reconstruction is in place. Coronal (top left), Axial (top right) and Sagittal (bottom left) multiplanar reconstructed (MPR) views of CT data. The 3D model constructed from CT data is shown in the bottom right corner.

Case C – Cerebellar hypoplasia

Patient description

A 33 year old male with complex foot deformity in the right foot resulting from cerebellar hypoplasia consisting of a cavus foot, supination of the forefoot and clawing of all toes. Complex foot deformity resulting from cerebellar hypoplasia in the contralateral foot has been surgically corrected at another hospital.

Treatment plan

Corrective surgery of case C has not occurred yet. The treatment plan is similar to that of case B and consists of a forefoot reconstruction aiming to eliminate clawing of all toes without virtual planning according to the Jones procedure followed four to six weeks later by midfoot reconstruction guided by virtual planning. The aim of corrective surgery is to reconstruct the longitudinal arch and restore the forefoot into a plantigrade orientation by execution of a closing wedge osteotomy.

Medical imaging

Weightbearing radiographs were acquired preoperatively of the right foot in lateral and DP view (Figure2.7). CT imaging of the foot was acquired with the foot set in a neutrally aligned position using a total contact cast. (Figure 2.8)

Application in this thesis

Neutral preoperative CT data was used in the case study described in chapter 5 regarding the design of a patient specific guide.

Figure 2.7: Weightbearing radiographs in lateral (left) and DP (right) view of the preoperative foot of case C

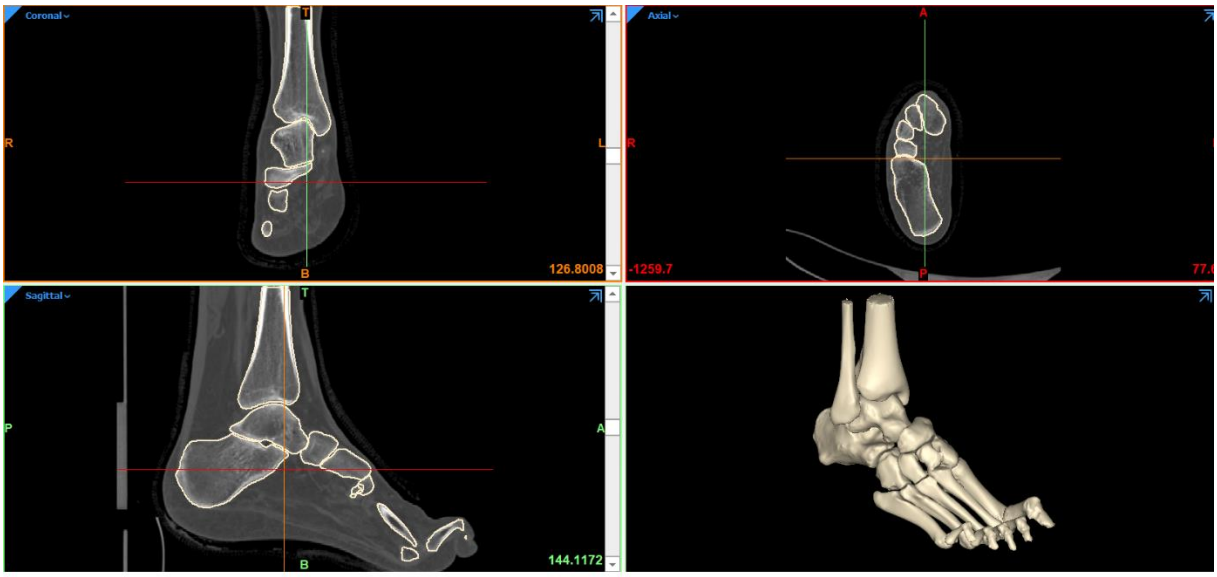

Figure 2.8: CT data of the preoperative foot of case C, neutrally aligned using a total contact cast. Coronal (top left), Axial (top right) and Sagittal (bottom left) multiplanar reconstructed (MPR) views of CT data. The 3D model constructed from CT data is shown in the bottom right corner.

Case D – Spastic Cerebral Palsy

Patient description

A 58 year old female with complex foot deformity in the right foot caused by spastic hemiparesis resulting from Cerebral Palsy. The deformity consists of a talocalcaneal coalition in a varus alignment, cavus foot and supination of the forefoot. Due to the spastic hemiparesis and foot deformity, the patient drags with her right leg, trips often and has pain complaints in her hip and back.

Treatment plan

Corrective surgery of case D has not occurred yet. The treatment plan consists of a corrective triple arthrodesis guided by virtual planning. This correction consists of hindfoot correction to restore the talocalcaneal coalition to a neutral alignment, followed by a midfoot correction aiming to restore the longitudinal arch and restore the forefoot into a plantigrade orientation.

Medical imaging

CT imaging was acquired preoperatively of the foot in a supinely aligned position (Figure 2.9). As this CT data contained motion artifacts in the metatarsals and normal values of reference angles cannot be applied in virtual planning using a supinely aligned foot, CT data of the foot in a neutrally aligned position using a total contact cast was acquired additionally. (Figure 2.10)

Application in this thesis

Supine and neutral preoperative CT data were used in the case study described in chapter 3 regarding foot position during CT acquisition. Neutral preoperative CT data was also used in the case study described in chapter 5 regarding the design of a patient specific guide.

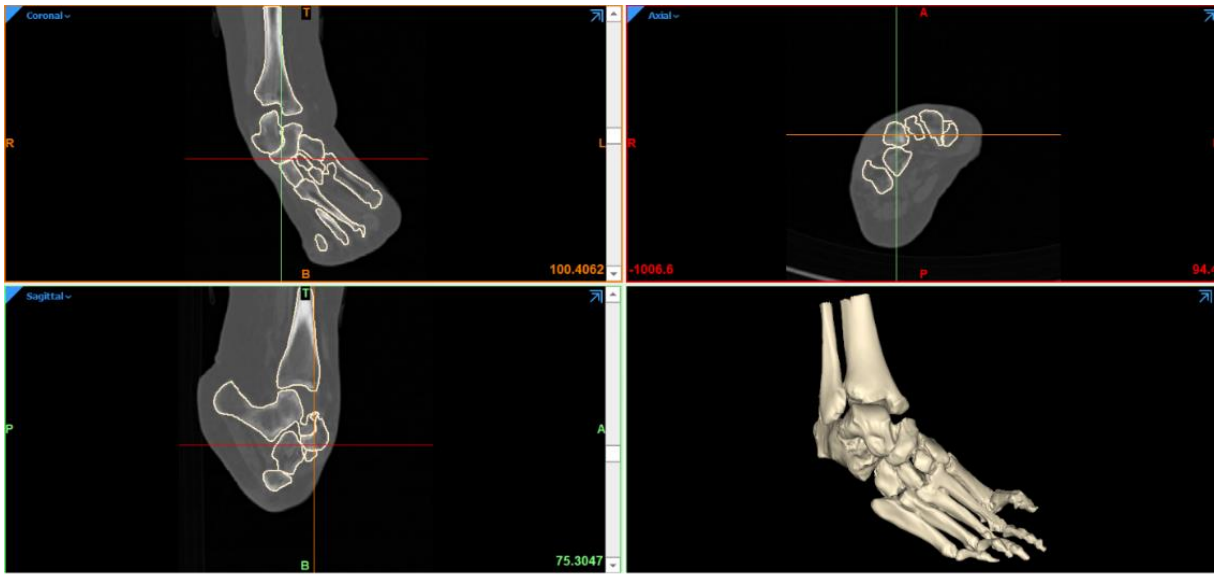

Figure 2.9: CT data of the supinely aligned preoperative foot of case D. Coronal (top left), Axial (top right) and Sagittal (bottom left) multiplanar reconstructed (MPR) views of CT data. The 3D model constructed from CT data is shown in the bottom right corner

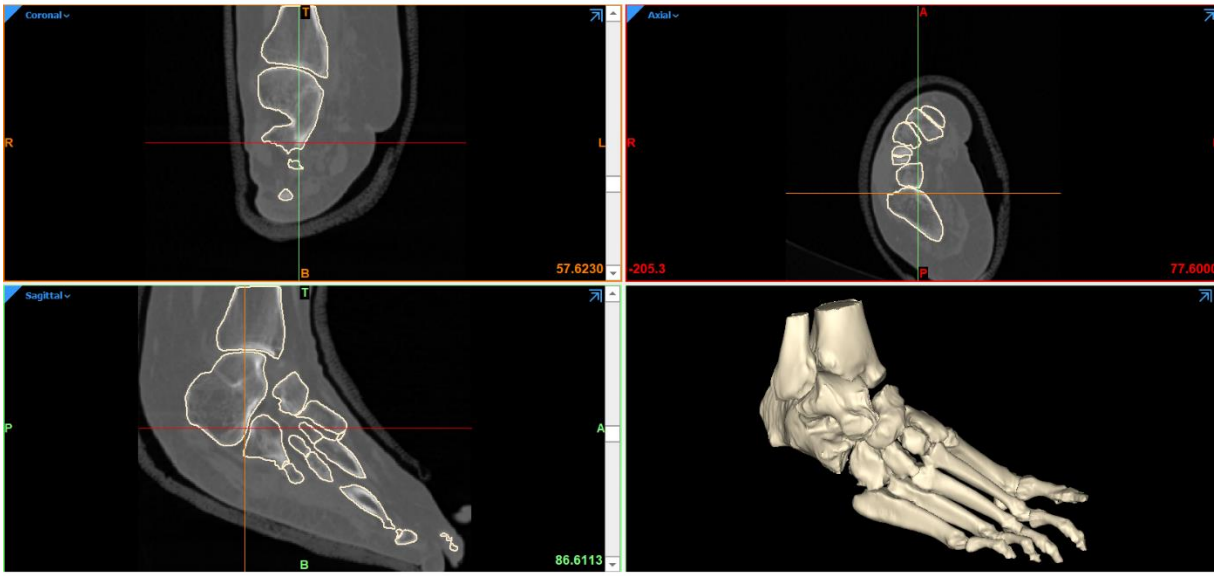

Figure 2.10: CT data of the preoperative foot of case D, neutrally aligned using a total contact cast. Coronal (top left), Axial (top right) and Sagittal (bottom left) multiplanar reconstructed (MPR) views of CT data. The 3D model constructed from CT data is shown in the bottom right corner.

Chapter 3 – Obtaining a 3D foot model to use during virtual planning

Introduction

The multiplanar nature of complex foot deformity cannot be completely understood from 2D imaging. Due to its 3D nature, Computed Tomography (CT) is considered the best modality for imaging complex foot deformity. (13,15) Additionally, it offers the possibility of creating a virtual 3D model of the affected foot, which can be used for virtual planning of corrective surgery. (15–17) As soft tissue interactions cannot be predicted virtually, planning of corrective foot surgery is limited to rigid foot deformities, which can only be corrected by osseous interventions. (14) In other orthopaedic applications, the mirrored contralateral unaffected side is used as template during virtual planning. (15) In complex foot deformities, however, the contralateral side is often affected and cannot be used as template during virtual planning. Therefore, virtual planning is based on restoring the reference angles described in literature.

The reference angles described in literature are measured in 2D weightbearing radiographs. To enable the use of these reference angles during virtual planning, CT data would ideally be acquired of the weightbearing foot. (13) Considering the non weightbearing position during surgery, on the other hand, preoperative imaging is ideally acquired in a non weightbearing position to ensure reliable virtual planning. (14,20) Richter et al. and Broos et al. both studied the influence of weightbearing on foot alignment by comparing reference angles in weightbearing and non-weightbearing neutrally positioned feet using a weightbearing cone-beam CT in patients and healthy volunteers respectively. Both studies described significant differences in measured angles between weightbearing and non-weightbearing neutrally positioned feet. (13,21) The weightbearing reference angles can, therefore, not be used directly in assessing CT data of supinely positioned feet.

To overcome this problem, Broos et al. introduced a new set of reference angles describing the healthy non-weightbearing neutrally aligned foot based on measurements in 40 healthy feet. (13) These reference values were added to Appendix A. To enable the use of these new reference angles during virtual planning, CT acquisition should be executed on a neutrally positioned non-weightbearing foot. This can be achieved by using a weightbearing CT scanner, as demonstrated by Broos et al, or by manual redressing of the foot into a neutral position. At Medisch Spectrum Twente (MST), a weightbearing CT scanner is not available. Therefore, manual redressing of the foot is applied to obtain a neutrally aligned foot. Setting the foot in a neutral position after manual redressing can be executed using a foot hold or a total contact cast. The use of a total contact cast is preferred over a foothold, as it ensures a maximum achievable neutral alignment during the entirety of CT acquisition even in case of spastic disease.

Considering the rigid nature of complex foot deformities, the question is raised whether the maximum achievable neutral alignment differs from the natural supine alignment and, therefore, whether manual redressing is necessary during preoperative imaging of rigid complex foot deformity. Therefore, the aim of this case study was to investigate the influence of manual redressing on the foot alignment in rigid foot deformity in two patients. This to determine the best foot position during preoperative CT imaging, and to enable the use of reference angles during virtual planning.

Materials and Methods

Patient description

For this case study, two patients witch complex foot deformity were included: cases B and D. All CT data was acquired at MST using a Somatom Definition Flash CT system (Siemens).

Case B was a 55 year old male with Charcot foot resulting from diabetic polyneuropathy in his right foot. Surgical correction was executed in two phases: forefoot reconstruction and midfoot reconstruction six weeks later. Supine CT data was acquired preoperatively, neutral CT data was acquired between the forefoot and midfoot reconstruction.

Case D was a 59 year old female with complex foot deformity resulting from spastic Cerebral Palsy in her right foot. Surgical correction has not been executed yet. Both supine and neutral CT data was acquired preoperatively.

Comparison of foot alignment

Comparison of foot alignment between the natural supine and maximum achievable neutral position was based on measurement of the non-weightbearing 2D reference angles described by Broos et al. (13). 3D models were obtained via semi-automatic segmentation of CT data in Materialise Mimics software (version 23.0), following the protocol included in Appendix B. In Materialise 3-Matic software (version 15.0), 3D models of the neutral and supine feet were visualized and used for measurement of reference angles. The 3D models were rotated manually until the talus was in an anatomical position to ensure correct projection planes for measurement of reference angles. Measurement of the reference angles was executed in dorsoplantar (DP) and lateral sketches. The reference lines needed for measurement of the reference angles were determined in the sketches as shown in Figure 3.1. Within-subject comparison of foot alignment was based on the reference angles measured in degrees by one observer.

Results

Figures 3.2 and 3.3 show the supine (creme) and neutral (grey) feet of case B and case D respectively, overlapping each other in the Talus in superior, lateral and medial view. Clearly visible in the virtual 3D representations of case B are the difference between the feet resulting from the forefoot reconstruction and the equinus of the supine foot. Clearly visible in the virtual representations of case D are the pre-existing talocalcaneal coalition and supination of the forefoot. Table 3.1 shows the measured reference angles of both cases. Due to the forefoot reconstruction in case B and pre-existing talocalcaneal coalition in case D, the results marked with a star could not be compared within the case.

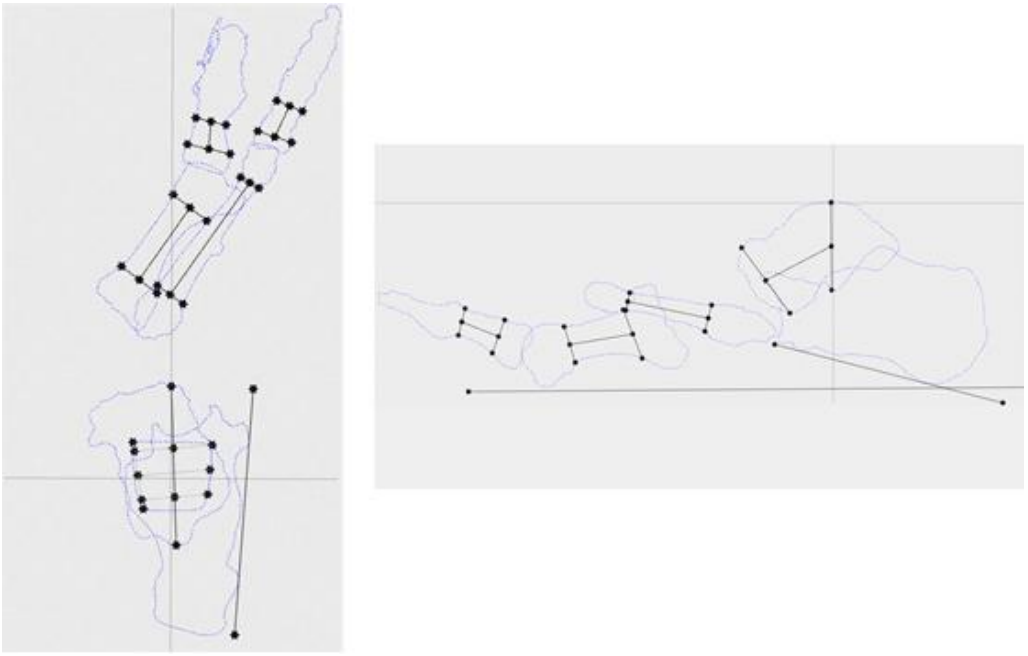

Figure 3.1: Dorsoplantar (left) and lateral (right) sketches including reference lines used in measurement of the reference angles in the neutral foot of case B

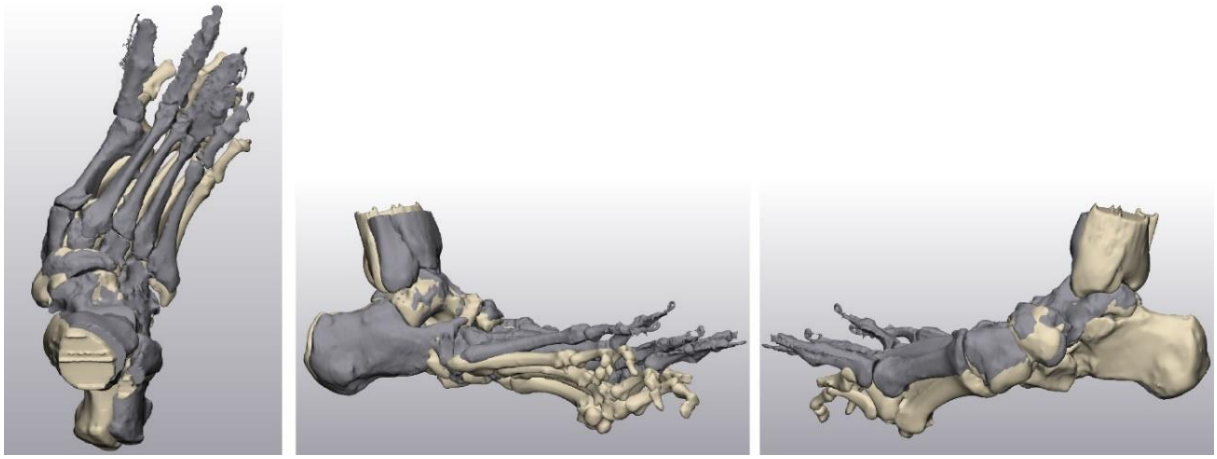

Figure 3.2: Supine (creme) and neutral (grey) foot of case B overlapping in the Talus in superior (left), lateral (middle) and medial (right) view. Clearly visible are the forefoot reconstruction and equinus of the supine forefoot.

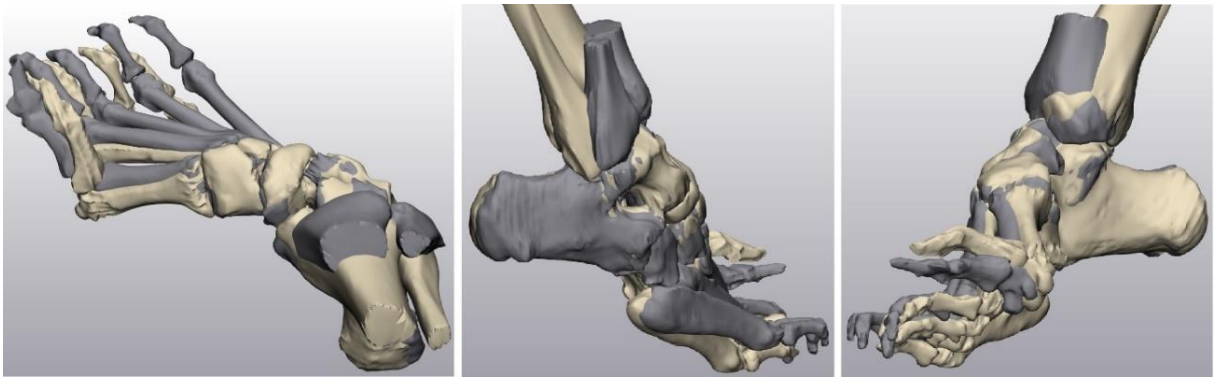

Figure 3.3: Supine (creme) and neutral (grey) foot of case D overlapping in the pre-existing talocalcaneal coalition in superior (left), lateral (middle) and medial (right) view. Clearly visible is the pre-existing talocalcaneal coalition and supination of the forefoot

Table 3.1: Measured reference angles in degrees in dorsoplantar (DP) and lateral planes for CT data acquired of natural supinely aligned and manual redressed neutrally aligned feet of cases B and D.

Angle	Plane	Case B Neutral	Case B Supine	Absolute difference	Case D Neutral	Case D Supine	Absolute difference
Calcaneal pitch	*Lateral*	14.5	17.7	3.2	18.3	21.8	3.5
Talocalcaneal angle	*DP*	6.1	11.6	5.5	*	*	*
Talocalcaneal angle	*Lateral*	41.8	35.3	6.5	*	*	*
Angle Talus-MT1	*DP*	36.8	42.7	5.9	96.1	82.6	13.5
Angle Talus-MT1	*Lateral*	17.9	7.8	10.1	45.8	69.3	23.5
MT1 – Proximal phalange 1	*DP*	*	*	*	49.8	78.7	28.9
MT1 – Proximal phalange 1	*Lateral*	*	*	*	92.8	51.7	41.1
MT2 – Proximal phalange 2	*DP*	*	*	*	48.6	57.4	8.8
Intermetatarsal angle	*DP*	0.2	1.9	1.7	8.1	11.5	3.4
MT5 – ground	*Lateral*	-12.1	-9.8	2.3	-8.7	8.5	17.2
MT5 – calcaneus	*Lateral*	2.7	7.9	5.2	9.5	30.4	20.9

**Results marked with a star were not usable in comparison due to forefoot reconstruction and pre-existing talocalcaneal coalition*

Discussion

This case study compared foot alignment in the natural supine position and the maximum achievable neutral position in rigid foot deformities based on non-weightbearing reference angles. We showed that foot alignment differs between the natural supine position and the manual redressed maximum achievable neutral position, even in rigid foot deformities. Differences in foot alignment are most prominent in fore- to hindfoot alignment, consisting of pes equinus and eversion in case B and pes equinus and inversion in case D.

The outcome of this study is comparable to that of Richter et al., who described significant differences between neutral and supine non weightbearing feet in 30 patients. (21) The foot pathologies present in these 30 patients were not taken into account by Richter et al. in processing the measured reference angles. Therefore, the research question regarding rigid foot deformities was still relevant to study with regards to the use of CT acquisition for virtual planning of complex foot surgery.

Differences between supine and neutral feet are discernible in all measured reference angles, but are most prominent in fore- to hindfoot alignment and forefoot alignment. As rigidity in complex foot deformity is often based around the mid- and hindfoot, differences in hindfoot alignment were expected to be less prominent. However, the measured values do show differences in hindfoot alignment between neutral and supine feet. This could be indicative of measurement error or intra-observer variability, which should be studied in further research.

As differences between supinely and neutrally aligned feet are most prominent in fore- to hindfoot alignment, differences in calcaneal inclination angle were not expected. The calcaneal inclination angle is the angle between the floor and the longitudinal axis of the calcaneus in lateral view. The floor is defined as the plane connecting the calcaneal tuberosity, medial sesamoid bone and the fifth metatarsal head. If foot alignment in rigid foot deformity would not be influenced by manual redressing, the floor and therefore the calcaneal inclination would not differ between supinely and neutrally aligned feet. However, due to the different fore- to hindfoot alignment, the orientation of the floor differs between both feet. This accounts for the difference between the measured calcaneal inclination angles and indicates the importance of manual redressing in rigid foot deformities.

The difference between neutral and supine feet in all measured reference angles can be explained in two ways. On the one hand, it can be caused by differences in projections of bones due to the change in foot alignment of the multiplanar deformity by manual redressing. These differences in projections could cause different reference lines leading to differences in measured reference angles. On the other hand, it can be caused by differences in the determined reference lines. Determination of the reference lines is executed manually guided by auxiliary lines. Determination of these auxiliary lines, however, is also manual and prone to minor differences between the two cases.

Measurement of reference angles is usually executed in weightbearing radiographs, of which the projection plane is determined based on the surface anatomy of the foot. Projection planes for measurement of reference angles in the virtual 3D model are determined based on the osseous anatomy. As weightbearing radiographs were not available for both described cases, projection planes in this study were based on the talar anatomy as described in literature. Likely, the orientation of the talus in these two cases is not comparable to the described normal weightbearing orientation. Therefore, the chosen projection planes might not be suitable for comparison of reference angles. Further research should be executed to determine the best way

In conclusion, manual redressing of rigid foot deformities using a total contact cast results in a foot alignment differing from the supine foot alignment. Combining the results of this case study with the

results of the case studies executed by Richter et al. (21) and Broos et al. (13), it is advisable to position the foot in the maximum achievable neutral alignment when acquiring CT data for virtual planning of complex foot surgery to enable the use of non-weightbearing reference angles during virtual planning.

Chapter 4 – Virtual planning of complex foot surgery – a case study

Introduction

Surgical correction of foot alignment is necessary in complex foot deformity to regain a plantigrade and stable foot, to prevent ulcerations and to enable mobility by bespoke footwear (6,11,22,23). Assessment of the deformity and preoperative planning are currently based on reference angles measured in 2D weightbearing radiographs. (7,8) In addition to the 2D radiographs, 3D CT imaging is currently used at MST to create a virtual 3D model of the osseous anatomy of the foot. This model is then 3D-printed to aid the orthopaedic surgeon in understanding the deformity, anticipating on the necessary corrections and informing the patient. (24) This 3D model could furthermore be used for virtual planning of the corrective surgery (14,18).

Virtual planning has proven useful in several other orthopaedic applications, such as spinal surgery, malunion correction and (knee) arthroplasty. (19) Reported benefits of virtual planning include shorter operation duration, a decrease in intraoperative radiation and, most importantly, improved anatomical outcome of the surgical procedure. (18,19) The use of virtual planning in corrective foot surgery with the additional use of a PSG has been described in three case studies. Indications for correction were cavus foot and Charcot foot, which were corrected via closing wedge osteotomy. (14,19,25) We found no reports on the effect of using virtual planning without application of a PSG. However, virtual planning itself may already have a positive effect on the outcome of complex foot surgery. To determine the effect of virtual planning alone on the execution of the planned correction, we have applied virtual planning in two patient cases, one retrospectively and one prospectively, and compared foot anatomy and alignment between preoperative foot, planned result and postoperative result.

Materials and methods

Patient description

Two patients were included in this case study: cases A and B. CT data was acquired at MST using a Somatom Definition Flash CT system (Siemens).

Case A was a 30 year old female with a postoperative malunion after triple arthrodesis in the right foot. The earlier triple arthrodesis led to fusion of the calcaneus, talus, navicular and cuboid bones with malposition in varus supination and adduction. Surgical correction was executed according to the current clinical practice, therefore surgery was not guided by virtual planning. Virtual planning of case A was executed retrospectively to determine the possible change in foot anatomy. Preoperative CT data was acquired with the foot in a supine position. Postoperative CT data was acquired at 2 months follow-up with the foot set in a neutral position using a total contact cast.

Case B was a 55 year old male with Charcot foot resulting from diabetic polyneuropathy in the right foot. Surgical correction was executed in two phases: forefoot reconstruction without virtual planning following the Jones procedure and midfoot reconstruction with the addition of virtual planning. Virtual planning for case B was executed prospectively, therefore surgery was guided by the virtual planning in combination with intraoperative radiographic imaging. The preoperative CT data used in virtual planning of the midfoot reconstruction was acquired after forefoot reconstruction with the foot set in a neutral position using a total contact cast. Postoperative CT data was acquired at 4 months follow-up with the foot in a supine position.

3D modelling and virtual planning

Virtual 3D models were obtained in Materialise Mimics software (version 23.0) by semi-automatic segmentation of preoperative CT data following the segmentation protocol added in Appendix B.

Preoperative CT data of case A was acquired with the foot in a supine position, as virtual planning was not applied in this case. Considering that postoperative CT data was acquired with the foot in a neutral position and reference angle normal values cannot be applied in a supinely aligned foot, manual realignment of the preoperative foot was necessary to obtain a neutrally aligned foot to use during retrospective virtual planning. The neutrally aligned postoperative CT data of case A was used as template for this realignment. The preoperative foot was relocated to coincide with the postoperative foot in the pre-existing coalition. Realignment was executed by registration of the tibia and fibula to the postoperative location and manual manipulation of the cuneiform bones and forefoot. The manual realignment was discussed with and approved by an orthopaedic surgeon before virtual planning of the midfoot reconstruction. Figure 4.1 shows the preoperative supine foot and the preoperative realigned foot and both in combination with the postoperative neutral foot.

Virtual planning for both cases was executed to obtain the planned result in Materialise 3-Matic software (version 16.0) following the virtual planning protocol added in Appendix C. As discussed in chapter 3, a healthy contralateral side is often not available to use as template during virtual planning of complex foot surgery. Therefore, virtual planning in this case study is based on realignment of the third metatarsal with the calcaneus in DP view as indicated by the orthopaedic surgeon and restoring Meary's angle to the normal value described by Broos et al. (13) in lateral view. For both cases, surgical correction of the complex foot deformity consisted of a closing wedge consisting of two osteotomies. In case A, the initial osteotomy was planned according to Chopart through the pre-existing collation located at the original distal calcaneus and talus. The second osteotomy was also planned through the calcaneus and talus, located more proximal from a posterolateral approach as shown in Figure 4.2. In case B, the initial osteotomy was planned according to Chopart through the distal calcaneus and talus. The second osteotomy was planned more proximal through the talus from a posteromedial approach as shown in Figure 4.3.

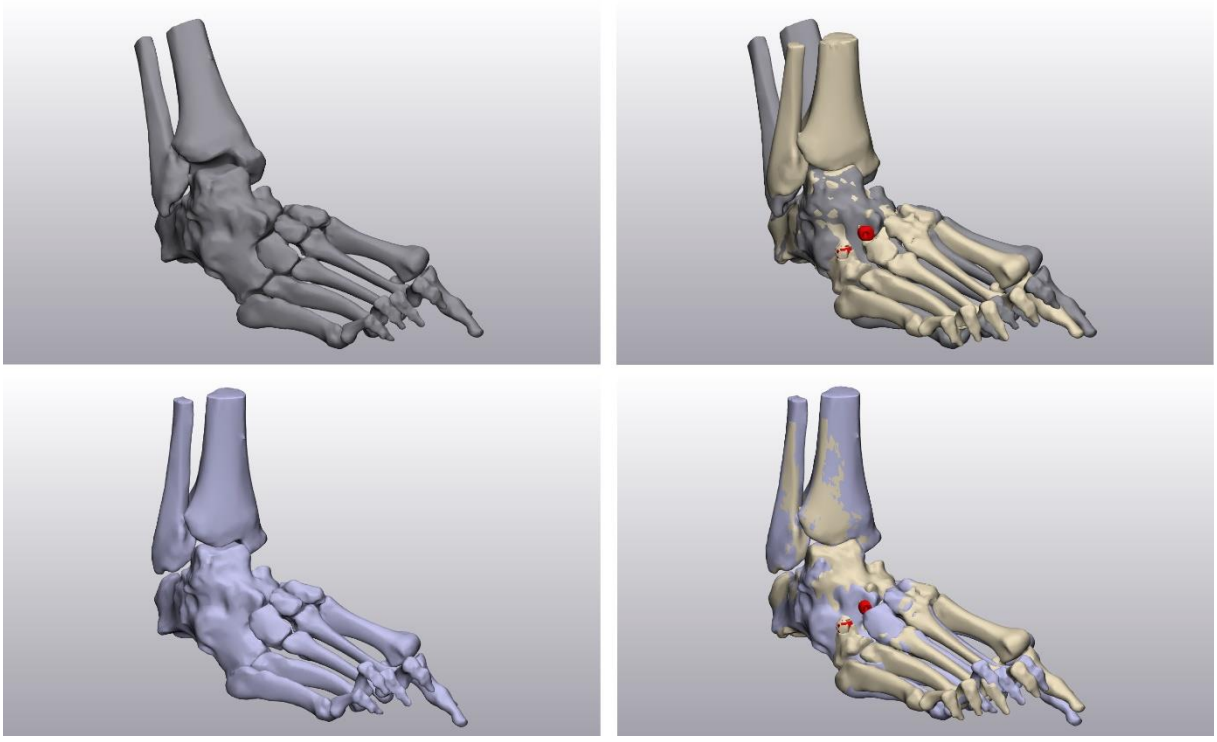

Figure 4.1: 3D models of case A, showing the original preoperative foot in grey (top left), neutrally realigned preoperative foot in lilac (bottom left) and each of these combined with the postoperative foot in creme (right), which was used as template for realignment

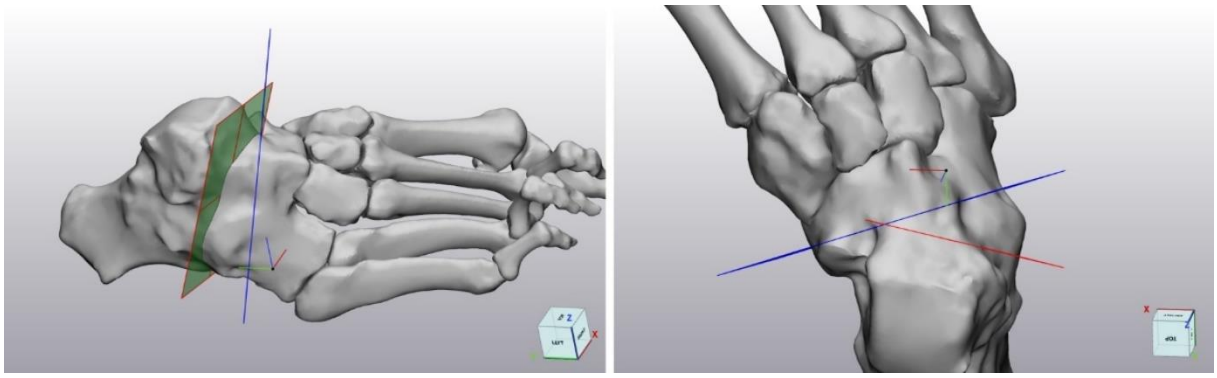

Figure 4.2: Virtual planning of closing wedge osteotomy in case A seen from lateral view (left) and superior view (right). The initial osteotomy is planned according to Chopart through the location of the distal calcaneus and talus. The second osteotomy is planned more proximal through the original calcaneus and talus from a posterolateral approach.

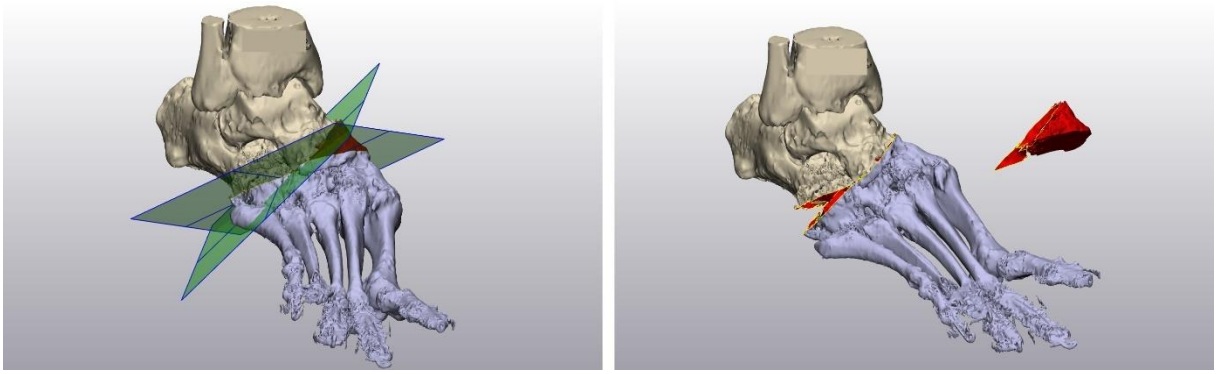

Figure 4.3: Virtual planning of closing wedge osteotomy in case B. Results of virtual planning of case B are a virtual model of the preoperative foot with indicated osteotomy planes (left) and a virtual model of the planned result (right). The initial osteotomy is planned according to Chopart through the distal calcaneus and talus. The second osteotomy is planned more proximal through the talus from a posteromedial approach.

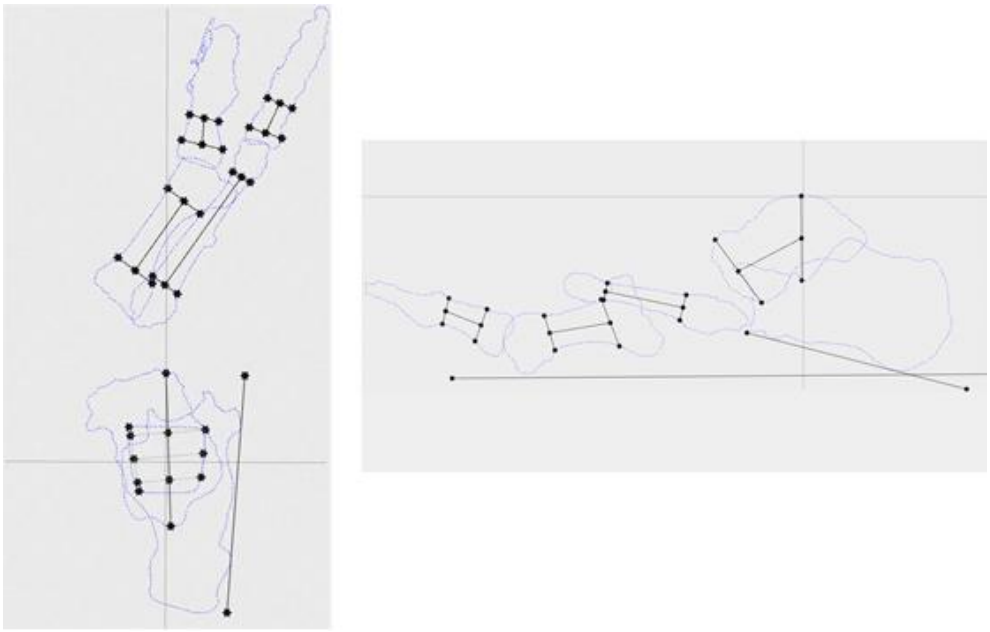

Figure 4.4: Sketches in DP (left) and lateral (right) view including bone outlines and reference lines, which were used in measurement of reference angles of the preoperative foot in case A

Pre- and postoperative foot anatomy

The within-subject pre- to postoperative change in foot anatomy was evaluated in both cases. The planned result was compared to the surgical result based on measured reference angles. Measured reference angles were compared 1) pre- to postoperative, 2) preoperative to planning and 3) all against reference values. The measured angles in DP view were in both cases Meary's angle, the Talocalcaneal angle (TCA DP) and the Calcaneal-second metatarsal angle (CM2). The measured angles in lateral view were Meary's angle, the Talocalcaneal angle (TCA lateral), the Calcaneal inclination angle (CIA) and the Djian-Annonier angle (DA). All reference angles were measured in degrees in Materialise 3-Matic software (version 16.0). Two sketches were created for each virtual model: one in DP view and one in lateral view. The outlines of relevant bones were imported and projected in these sketches for determination of the reference lines (Figure 4.4).

Results

The measured reference angles of case A and B are shown in Tables 4.1 and 4.2 respectively. Figures 4.5 and 4.6 show the preoperative foot, planned result and postoperative foot of case A in superior, lateral and posterior view and of case B in superior, medial and posterior view respectively. What can be seen in these results is that the measured postoperative angles in case B are closer to the planned angles than in case A. Also, the planned result is a more extreme correction than the surgical outcome in both cases.

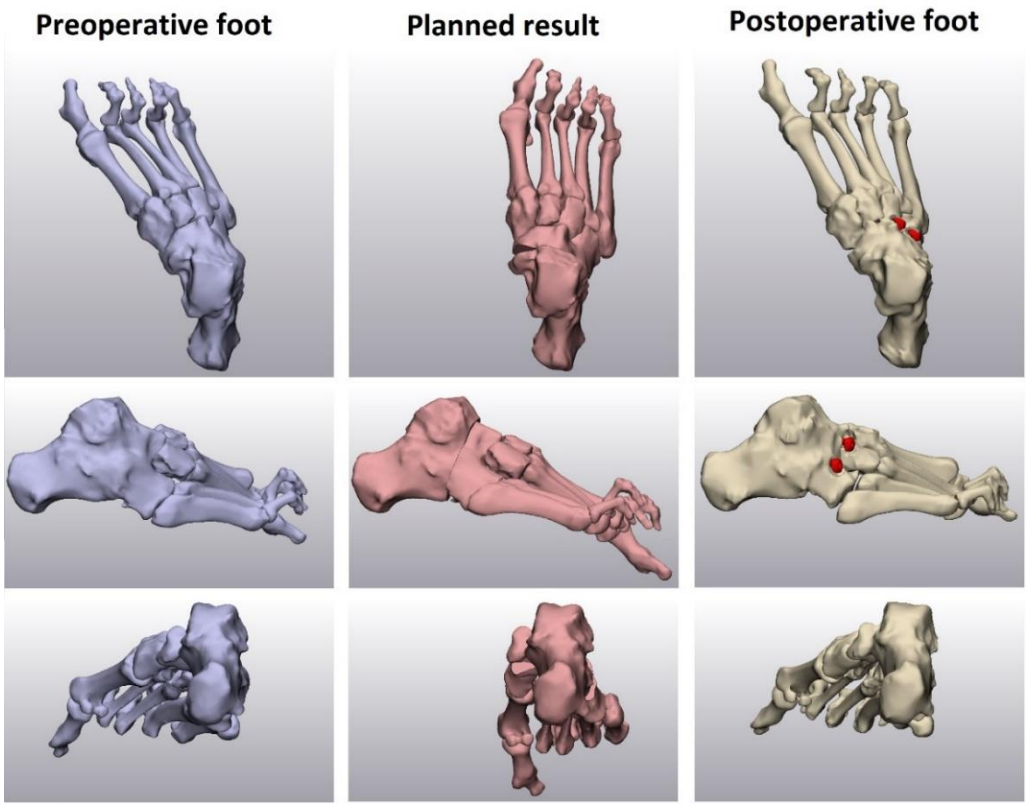

Figure 4.5: 3D models of the preoperative foot, planned result and postoperative foot of case A in superior (top), lateral (middle) and posterior (bottom) view

Table 4.1: measured values of reference angles in degrees in case A.

Angle	Plane	Normal value	Preoperative	Planned result	Postoperative result
Meary's angle	DP	3-11	45,69	11,47	31,73
Talocalcaneal angle	DP	15-27	1,97	3,37*	3,74*
Calcaneal-MT2	DP	3-4	49,61	12,1	38,15
Calcaneal inclination angle	Lateral	13-23	14,82	16,58	12,48
Meary's angle	Lateral	2-10	7,47	4,59	7,01
Talocalcaneal angle	Lateral	45	38,21	42,45*	30,66*
Djian-Annonier	Lateral	120-130	115,67	114,76	127,14

**Values of planned result and postoperative foot are similar due to a pre-existing coalition of talus, calcaneus, navicular and cuboid.*

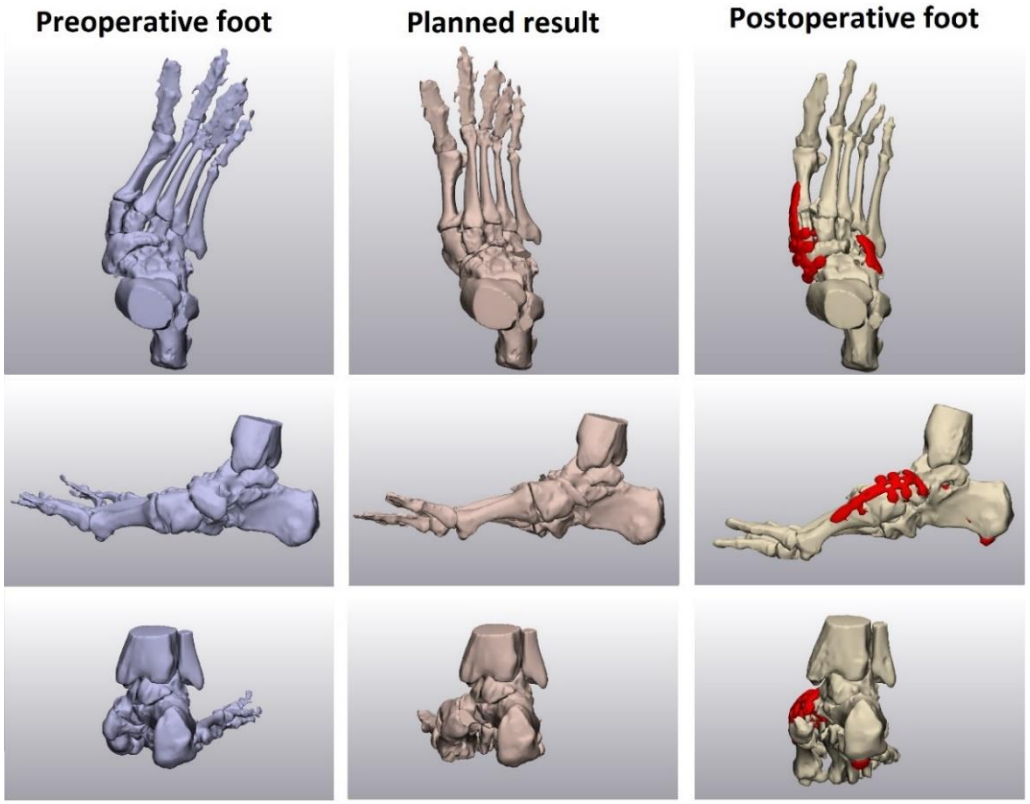

Figure 4.6: 3D models of the preoperative foot, planned result and postoperative result of case B in superior (top), medial (middle) and posterior (bottom) view

Table 4.2: Measured values of reference angles in degrees in Case B.

Angle	Plane	Normal value	Preoperative	Planned result	Postoperative result
Meary's angle	DP	3-11	61,76	29,83	33,92
Talocalcaneal angle	DP	15-27	29,6	29,81	30,82
Calcaneal-MT2	DP	3-4	30,97	1,29	8,24
Calcaneal inclination angle	Lateral	13-23	31,22*	31,43*	15,59*
Meary's angle	Lateral	2-10	-14,89	-8	1,42
Talocalcaneal angle	Lateral	45	36,75	36,36	37,94
Djian-Annonier	Lateral	120-130	131,52	129,5	126,3

**Differences in calcaneal inclination angle can be explained by the difference between the neutral preoperative and supine postoperative foot alignment.*

Discussion

This case study was performed to determine the potential added value of using virtual planning in the preoperative planning of complex foot surgery. The results show an improvement of foot anatomy in both the virtually planned result and the postoperative result in all measured reference angles in both cases.

Virtual planning of case A was executed retrospectively, after surgical correction was executed according to the current clinical practice without virtual planning. The postoperative result is an improvement in foot anatomy compared to the preoperative situation. At 9 months follow-up, mobilisation was possible with normal footwear in combination with arch support. The executed surgery, however, has not achieved correction of the reference angles into the normal value range. The planned result shows measured angles closer to or in normal value range. As reference angles describe the healthy foot alignment, corrective surgery ideally restores all reference angles into normal value range. This would guarantee correct weight distribution and a normal foot shape, thereby reducing chance of ulcerations and enabling mobilisation with normal footwear. The differences between the reference values measured in the planned result and the postoperative result indicate the possible further improvement of the postoperative result by the application of prospective virtual planning.

Virtual planning of case B was executed prospectively and used intraoperatively for guidance of the surgical correction. Based on measurement of reference angles, the postoperative result is an improvement in foot anatomy compared to the preoperative situation. At 9 months follow-up, mobilisation was initialized using a CROW walker to prevent new ulcerations or deformity. (26) The measured reference angles in the postoperative result show an improvement in foot anatomy similar to the planned result, which was expected as surgical correction of case B was aided by virtual planning. The 3D visualization increased understanding of the deformity and necessary corrections during virtual planning. Additionally, the virtual model of the preoperative foot with indicated osteotomy lines aided the orthopaedic surgeons intraoperatively in execution of the planned osteotomies. Like case A, the measured reference angles in the planned result were closer to the normal value range than the postoperative result. This difference between measured reference angles might be reduced by the implementation of PSGs. The use of PSGs in complex foot surgery has already been studied in a number of cases with successful results. (14,18,20) The implementation of PSGs could improve the translation of the virtual planning to the operation table and therefore, improve the surgical result of complex foot surgery even more than virtual planning alone.

Most of the measured reference angles in case B have similar values in the planned and postoperative result. The measured values of the calcaneal inclination angle are, however, very different. This difference can be explained by the fact that postoperative CT data was acquired with the foot in a supine position instead of a neutral position. As discussed in chapter 3, the difference in foot anatomy between supine and neutral alignment would result in a different plane defined as floor for measurement of the calcaneal inclination angle. Therefore, comparison of this reference angle is impossible between neutral and supine foot alignment. For future reference, it is advisable to perform all imaging in the neutral alignment when comparing preoperative and postoperative foot anatomy to ensure correct analysis of the result.

Seeing that case A has a pre-existing coalition of the calcaneus, talus, navicular and cuboid bones, the talocalcaneal angles should be similar in all measurements. However, the measured talocalcaneal angles differ in both DP view and lateral view between all measurements. This could indicate an intra-observer variability due to manual determination of the reference lines used in measurement of the reference angles. In future studies comparing foot anatomy based on measured reference angles, it

would be advisable to either develop an automatic method to determine the reference lines or calculate the intra-observer variability to increase the accuracy of the results.

In this case study, the reference angles determined in weightbearing X-rays are used in both virtual planning and postoperative analysis of the foot anatomy. The CT imaging used in creating the 3D model, however, is non-weightbearing. This difference was anticipated on by acquiring CT data of the foot in a neutral alignment, which is similar to the foot alignment during weightbearing. There are, however, studies showing the difference between weightbearing neutral and non-weightbearing neutral aligned feet when comparing weightbearing X-rays with weightbearing neutrally aligned CT and non-weightbearing neutrally aligned CT in patients and healthy volunteers (13,21). This indicates an error in this case study in both virtual planning and postoperative analysis, as this change in reference angles was not accounted for. Considering the non-weightbearing intraoperative situation, it would be advisable in future cases to use the non-weightbearing reference angles described by Broos et al. (13) during virtual planning.

In conclusion, an improvement in execution of complex foot surgery is indicated in the case where virtual planning was applied retrospectively. This can probably be achieved by application of prospective virtual planning. In the case where virtual planning was applied prospectively, the surgeon experienced a better understanding of the deformity and necessary corrections, and achieved an anatomical result with reference angles close to or in normal value range.

Chapter 5 – Designing a patient specific guide for complex foot surgery

Introduction

Complex foot surgery can be planned virtually using a 3D model created out of preoperative CT data. During virtual planning the osteotomies, translations and rotations needed for correction of the foot are determined based on restoring reference angles to normal values. This virtual plan already increases understanding of the deformity and comprehension of the necessary osteotomies. Translation from planning to operating table without intraoperative guidance, however, is difficult for the surgeon. This could lead to different and possibly less optimal, surgical results. Accurate translation of the virtual planning to the operating table would improve the execution of the planned correction and could improve the surgical result.

Translation of virtual planning to the surgical procedure can be achieved using patient specific guides (PSGs). PSGs are surgical instruments custom made to fit a patient's anatomy. Common PSG functions include screw placement, saw guidance and bone reposition guidance. (18,19) PSGs are commonly designed based on a virtual preoperative plan containing a 3D model of the anatomy with indicated surgical procedures such as osteotomy planes, drilling trajectories, screw placements and bone repositioning.

PSGs have been applied in the orthopaedic field for over 20 years and have documented advantages such as decreased surgical time, decreased exposure to radiation during surgery and increased accuracy of the intended procedure. Application of PSGs in the orthopaedic field include spinal surgery, (knee) arthroplasty and malunion corrections. (19) Even though complex foot surgery could benefit from the use of PSGs, they are not yet commonly applied in that field. Popescu et al. (18), Dagneaux et al. (14) and Sobrón et al. (20) all applied PSGs in complex foot surgery for a total of seven cases of midfoot deformity. In all studies, cutting guides were developed and applied during complex foot surgery with promising results, thereby indicating the possibility of implementing PSGs in complex foot surgery.

To enable in-house use of PSGs at MST, a design protocol should be developed containing general design guidelines for a PSG for complex foot surgery, which can be made case specific by using the patient's anatomy and intended surgery. The objective of this chapter was to develop such guidelines by determining prerequisites and designing and testing PSG prototypes for three clinical cases.

Materials and methods

Prerequisites for PSG design

The design of a PSG should combine the necessary structural and functional criteria with the surgeons' preferences while ensuring the sterilization of the finished product. Popescu et al. (18) have studied design guidelines for PSGs in the orthopaedic field as documented in literature and validated this information in multiple clinical cases including three foot deformities. This study resulted in a clearly documented list of guidelines for design and 3D printing of PSGs. These guidelines describe the structural criteria to obtain a robust and secure PSG. Functional criteria were defined in consultation with the orthopaedic surgeon. Combining the findings of Popescu et al. (18), restrictions provided by the supplier and the preferences of the orthopaedic surgeon, a list of prerequisites for PSG design was constructed, which are shown in Table 5.1.

Table 5.1: Prerequisites for design of a patient specific guide for complex foot surgery

Category	Prerequisites	Source
Structural criteria	A PSG must be manufactured in a facility that is compliant with ISO 13485 standards. The material of a PSG must be biocompatible and sterilizable according to ISO993, such as Polyamide 12 (PA12)	Hospital guidelines
	For intraoperative use, the PSG must be sterilizable. When manufacturing is outsourced to Oceanz B.V., sterilization is ensured up to the following part dimensions: The maximum part dimensions should be 240x190 mm For placement of black k-wires (diameter of 1.57 mm), the hollow cylinders should have a maximum height of 4 mm when using a wall thickness of up to 4 mm, or a maximum height of 10 mm when using a wall thickness of up to 2 mm. When using a part thickness of 4-10 mm, a cutting slot for saw guidance should have a maximum width of 1 mm. The wall thickness of saw guidance slots should be minimum 4 mm.	Supplier guidelines (Oceanz B.V.)
	To obtain a robust PSG, which will not be distorted by the printing and sterilization processes, the minimum part thickness should be 3.5 mm. For stable placement of k-wires through the PSG, a clearance between the outer border of the k-wires and the inner border of the hollow cylinders should be 0.15 mm. For a stable cutting guidance, the minimum hight of the saw guidance block should be 10 mm. For stable drilling guidance using hollow cylinders, the cylinders should have a minimum length of 20 mm and minimum outer diameter of 10 mm When defining a cutting trajectory by drilling through hollow cylinders and using an osteotome, the distance between these cylinders should be 5-10 mm.	Popescu et al. (18)
	For a unique and stable fit of the PSG, a 160-degree span of PSG over bone would ideally be used in guide seating. To account for periosteum, a clearance between bone surface and bottom surface of PSG of 0.1 - 0.2 mm should be included in the design	
	To ensure a secure fixation of PSG to bone, a minimum of 1 k-wire per bone is necessary. If possible, fixation would ideally be obtained using a minimum of 4 k-wires	
	When using separate cutting and repositioning guides, the location and orientation of K-wires should be the same in both guides.	
Functional criteria	To ensure the intended functionality after placement of the PSG, there should be zero remaining degrees of freedom. The PSG should lock the foot alignment in the same alignment as used in virtual planning. Placement of the PSG should ensure complete visualization of the wedge to be removed. Functions that should be included in the PSG are cutting guidance and repositioning guidance for correct execution of the intended translations and rotations. Using the repositioning guide, it should be possible to keep the forefoot stable in the right alignment while allowing flexibility in the transverse arch due to joint opening, for correct intraoperative determination of a second osteotomy plane. A repositioning guide should ensure sufficient bone-to-bone contact after repositioning of the forefoot into the planned orientation.	Surgeon

PSG development for clinical cases

Based on the prerequisites listed in Table 5.1, PSG prototypes were designed and 3D printed for three patient cases with rigid foot deformity (cases B, C and D). For each of these cases, a virtual 3D model was obtained from CT data and virtual planning was executed according to protocol (Appendices A1 and A2). Seven general PSG prototypes were designed in development of the PSG design protocol, which can be personalized to a patient's anatomy and intended surgery. The initial prototype design was based on virtual planning of case B. Adaptations in general PSG design were made based on feedback, new ideas and the introduction of cases C and D. In all developed PSG prototypes, the guide base was created by extruding a selected part of the bone surface for 4 mm, similar to Sobrón et al. (20)

Case B

Case B was a 55 year old male with Charcot foot resulting from diabetic polyneuropathy in his right foot. The deformity consisted of dysplasia of the navicular, pes planus with varus pronation of the forefoot and clawing of all toes. Correction of the complex foot deformity was executed in two phases: forefoot reconstruction according to the Jones procedure aiming to eliminate clawing of all toes followed by midfoot correction aiming to restore the longitudinal arch and realign the forefoot. Virtual planning of the midfoot aimed to correct the deformity using a closing wedge osteotomy. In closing the gap, the aim was to obtain sufficient bone-to-bone contact between hind- and forefoot to allow bone growth between the two resulting surfaces. Two osteotomies were planned from a medial and posteromedial approach. Figure 5.1 shows the 3D models of the preoperative foot with indicated osteotomy planes and of the planned postoperative foot, which were used in PSG design.

Five general PSG prototypes were developed based on virtual planning of case B. The first general PSG prototype was a cutting guide designed for correct execution of both osteotomies. This prototype was seated on the wedge to be removed (wedge), with cutting guidance blocks on either side of the PSG. (Figure 5.2A) During consultation with the orthopaedic surgeon, feedback indicated that a clear view of the wedge was desired during surgery. Adaptation of the initial design resulted in the second general PSG design consisting of two separate cutting guides located on either side of the wedge. (Figure 5.2B)

In the third general PSG prototype another type of cutting guidance was implemented, which was applied by Sobrón et al. in their PSG design. The sawblade was not guided by the PSG itself, but by three Kirschner wires (K-wires) placed parallel to the osteotomy plane. The PSG is used in placement of the K-wires and was removed before cutting. (20) Building on this, the third general PSG prototype consisted of a double cutting guide located on either side of the wedge with K-wire holes instead of a cutting block. (Figure 5.1C)

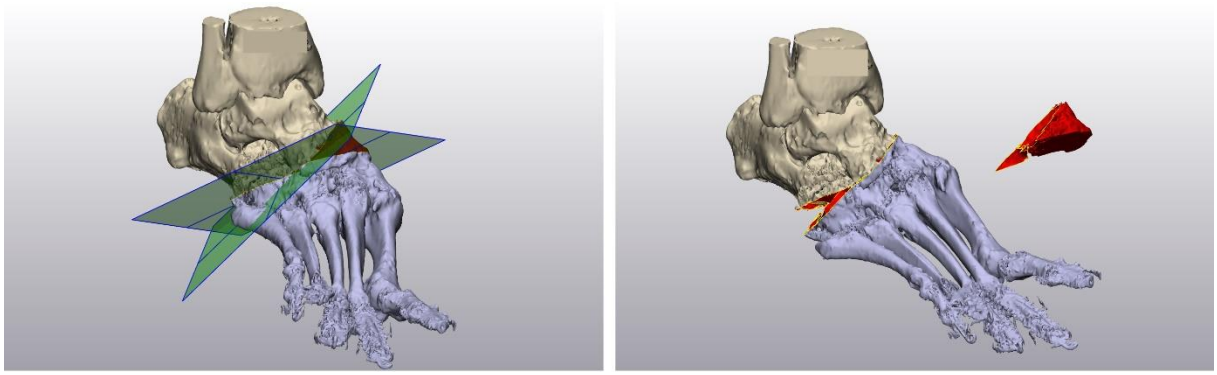

Figure 5.1: 3D models of case B showing the preoperative foot with indicated osteotomy planes (left) and the planned postoperative foot with removed wedge (right) which were used in PSG design

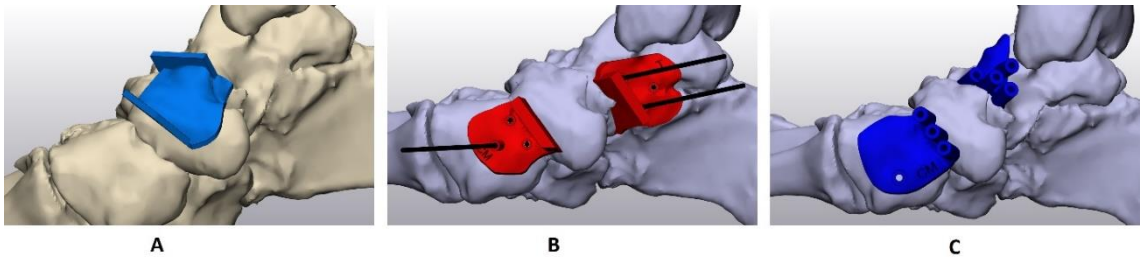

Figure 5.2: Prototypes developed based on case B. A) The first general prototype was a double cutting guide located on the wedge to be removed with cutting guidance blocks B) The second general prototype was a double cutting guide located on either side of the wedge to be removed with cutting guidance blocks C) The third general prototype was a double cutting guide located on either side of the wedge, with hollow cylinders for placement of cutting guidance K-wires. The first three PSG prototypes only included cutting guidance.

Considering the prerequisite of repositioning guidance, the fourth general PSG design was an adaptation of the third prototype to implement repositioning guidance. When using a PSG for both cutting guidance and repositioning guidance, either two separate PSGs can be designed or one PSG with both functions. (18) When integrating repositioning guidance in the cutting guide, it is presumed that operating time, the error rate due to placement of a second PSG and manufacturing costs are all decreased. Therefore, a solution was sought to integrate the repositioning guide in the cutting guide. An example in literature combining the cutting and repositioning guide was executed by Yang et al. (27) They applied PSG with the combined cutting and repositioning guidance in medial opening wedge high tibial osteotomies. (Figure 5.3A) This integrated repositioning guide consisted of an aligning rod and two aligning holes connected to the cutting guide. When correct alignment of the bone fragments was achieved, the alignment rod fitted through both aligning holes, locking the correct alignment and fixation could be achieved. This principle was applied in the fourth prototype, using a K-wire as aligning rod. Considering the remaining degree of freedom when using one K-wire, two aligning holes were placed in a cylinder (alignment rod) to use as repositioning guide. Considering the prerequisite of the same foot alignment intraoperatively as during virtual planning, a bridge was added to connect the two guide bases and lock the orientation between them. This bridge must be removed before repositioning of the forefoot. (Figure 5.3B)

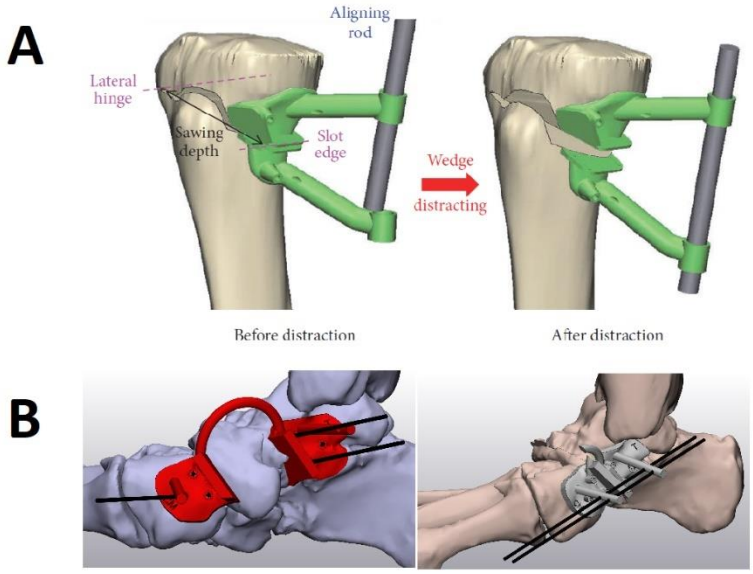

Figure 5.3: A) PSG designed by Yang et al. (27) for medial opening wedge high tibial osteotomies with implemented repositioning guidance. B) Our implementation of the technique described by Yang et al. in the fourth general PSG prototype for complex foot surgery

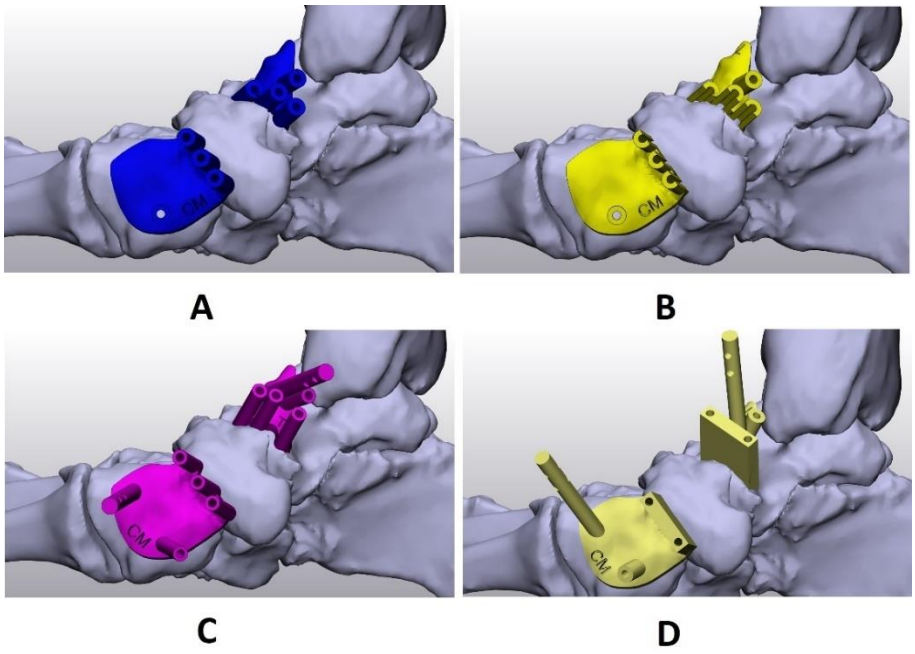

Figure 5.4: Designed PSG prototypes for complex foot surgery in case B A) The third general prototype PSG using k-wire guided cutting, which cannot be used for intraoperative repositioning due to overlap between hollow cylinders and opposing guide base and hollow cylinders. B) First solution for both k-wire guided cutting and intraoperative repositioning: hollow cylinders cut through at osteotomy plane resulting in semi-circles C) Second solution for both k-wire guided cutting and intraoperative repositioning: the fifth general PSG prototype is an interlocking system of hollow cylinders D) The fifth general PSG prototype with cutting guidance blocks instead of k-wire guided cutting

The third prototype PSG was designed using the anatomy of the preoperative foot. Repositioning guidance, however, should be designed using the anatomy of the planned postoperative foot to ensure correct alignment of the k-wire holes in the alignment rods. When repositioning the forefoot with the fixated distal part of the third PSG prototype from the preoperative orientation to the planned postoperative orientation for design of the repositioning guidance, the hollow cylinders for placement of saw guidance K-wires overlapped with the proximal guide. Therefore, complete intraoperative repositioning of the forefoot would be impossible using this PSG design. Two solutions were found to enable both K-wire guided cutting and repositioning guidance combined in one PSG. First, the K-wire holes were simply cut off at the osteotomy level, resulting in semicircles. (Figure 5.4B) This would, however, reduce the stability for K-wire placement and was rejected straight away. Second, PSG design was executed using the planned postoperative result instead of the preoperative foot. To enable both K-wire guided cutting and solid repositioning, an interlocking system was created. Joining guide bases were created on each side of the wedge. Holes for placement of K-wires for cutting guidance were placed alternately on both guide bases. Overlap of these holes with the other guide base were prevented by removing part of the guide base, so the hole will lock into position. (Figure 5.4C) For comparison of K-wire guided cutting and cutting blocks, the fifth general PSG prototype was also created with cutting blocks. (Figure 5.4D)

Case C

Case C was a 33 year old male with complex foot deformity resulting from cerebellar hypoplasia in his right foot consisting of a cavus foot, supination of the forefoot and clawing of all toes. Correction of the complex foot deformity will be executed in two phases: forefoot reconstruction aiming to eliminate the clawing of all toes according to the Jones procedure and midfoot reconstruction aiming to restore the longitudinal arch and realign the forefoot. Virtual planning was executed for the midfoot correction.

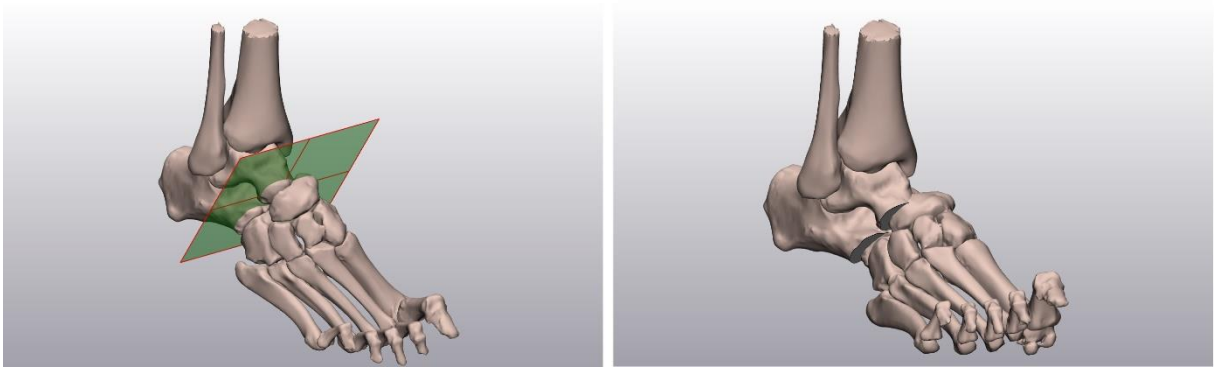

Figure 5.5: 3D models of case C showing the preoperative foot with indicated initial osteotomy plane (left) and the preoperative hindfoot with the forefoot in the planned postoperative orientation without execution of a second osteotomy (right) which were used in PSG design

Contrary to case B, sufficient bone-to-bone contact between hind- and forefoot could not be achieved when complete rigidity of the foot was assumed, due to a heightened and narrowed transverse arch resulting from the cavus deformity. When cutting through this deformed arch and rotating the forefoot, the transverse arch is placed under such an angle that sufficient bone-to-bone contact cannot be established without loss of foot length. Therefore, the second osteotomy plane could not be determined accurately during virtual planning. However, the assumption of complete rigidity is probably incorrect, as opening of joint capsules results in some flexibility and therefore change in the slope of the transverse arch. This flexibility is unpredictable and can only be assessed intraoperatively. Therefore, virtual planning consisted of determination of the initial osteotomy plane and realignment of the forefoot without determination of the second osteotomy plan. Figure 5.5 shows 3D models of the preoperative foot with indicated initial osteotomy plane and of the preoperative hindfoot with the forefoot in the planned postoperative orientation without execution of a second osteotomy.

Considering that the second osteotomy plane could not be determined in case C, a double cutting guide with integrated repositioning guide could not be developed. Most important in designing the new PSG prototype were the cutting guidance for the initial osteotomy and the repositioning guidance for obtaining correct alignment of the forefoot. Because hindfoot alignment can be fixated intraoperatively in neutral alignment using a k-wire, a cutting guide can be developed to ensure correct execution of the initial osteotomy in the same manner as earlier general prototypes. The second cutting guide has to be replaced by a repositioning guide. Therefore, the sixth general PSG prototype consists of a proximal cutting and repositioning guide combined with a distal repositioning guide. The second osteotomy has to be determined intraoperatively by the orthopaedic surgeon, parallel to the initial osteotomy guidance block. The cutting guide base for case C was located on the lateral side of the talus and calcaneus and followed the interior of the sinus tarsi. The alignment K-wires in the alignment rod were oriented parallel to the Calcaneal-third metatarsal line in DP view, to ensure correct alignment of the forefoot as base for the second osteotomy while allowing flexibility in the transverse arch. (Figure 5.6A)

The sixth general PSG prototype as designed for case C was 3D printed in dental SG resin for assessment of this general PSG prototype by one orthopaedic surgeon. In consultation with the orthopaedic surgeon, this prototype was scored using a 5-point Likert scale (poor, fair, good, very good, excellent) in four categories divided into several sub-categories. The categories are shown in Table 5.2. The cutting guide and the repositioning guide were scored separately.

Table 5.2: Categories for scoring of PSG prototypes by an orthopaedic surgeon

Category	Subcategories
Design	– Size – Sturdiness – Marks for placement – Alignment rod – Cutting block
Fitting	– Location – Unique fitting
Fixation	– Number of K-wires – Location of K-wires – Orientation of K-wires – K-wire placement guidance
Applicability	– General functionality – Usability

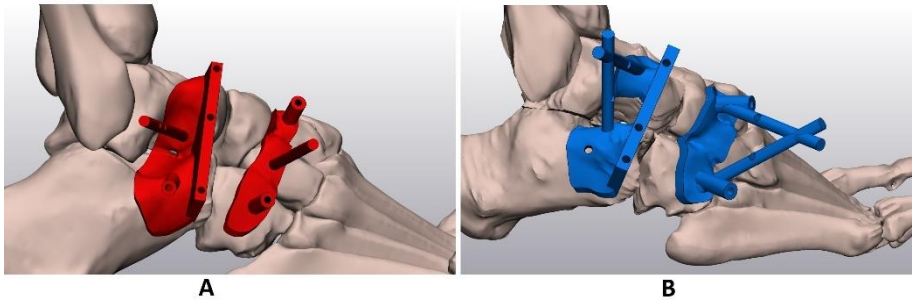

Figure 5.6: A) Sixth general PSG prototype as designed for case C B) Seventh general PSG prototype as designed for case D

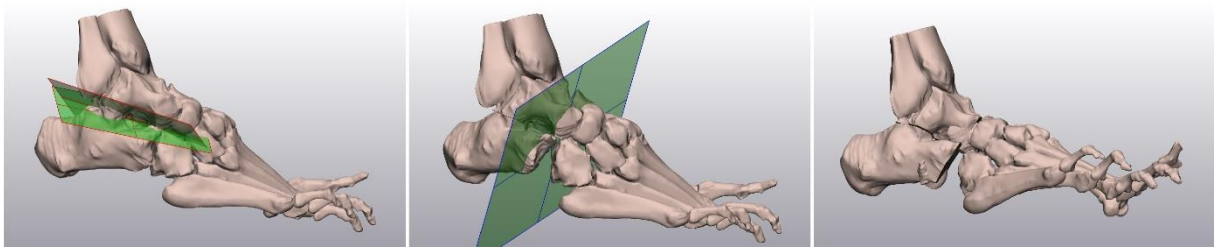

Figure 5.7: 3D models of case D showing the preoperative foot with indicated osteotomy planes for hindfoot correction (left), the preoperative foot after hindfoot correction with indicated initial osteotomy plane (middle) and corrected hindfoot with forefoot in planned postoperative orientation without executed second osteotomy (right), which were used in PSG design.

Case D

Case D was a 58 year old female with complex midfoot deformity of the right foot resulting from spastic cerebral palsy. The deformity consisted of a talocalcaneal coalition in varus deformity, cavus foot and supination of the forefoot. Virtual planning was executed for hind- and midfoot correction and aimed to restore the hindfoot into a neutral position, restore the longitudinal arch and realign the forefoot into a neutral position. Virtual planning consisted of hindfoot correction followed by midfoot correction. Like case C, sufficient bone-to-bone contact could not be established during midfoot correction and the second osteotomy plane could not be determined preoperatively. Figure 5.7 shows the 3D models of the preoperative foot, the preoperative foot after hindfoot correction and the corrected hindfoot with the forefoot in the planned postoperative orientation without execution of a second osteotomy.

The virtually planned hindfoot correction resulted in a clear gap between the repositioned talus and calcaneus. Therefore, the sixth general PSG prototype design had to be adapted. For the seventh general PSG prototype, the proximal guide base consisted of two separate bases connected by the cutting guidance block. To obtain an extra connection between the two bases and therefore increased stability in the cutting guide, the alignment rod was changed to an alignment triangle consisting of two crossing cylinders originating from the two separate guide bases. This had the additional benefit of increased stability in the repositioning guide compared to the single alignment rod. (Figure 5.6B)

The seventh general PSG prototype as designed for case D was printed in dental SG resin and assessed by the same orthopaedic surgeon in the same way as the sixth general PSG prototype as designed for case C.

Results

PSG design

Seven general PSG prototype designs for complex foot surgery were developed in this case study, which can be made case specific based on a patient's anatomy and intended surgery. A PSG design protocol was developed for design of the seventh prototype, using data of case C. This protocol can be found in Appendix E.

In vitro evaluation

The results of the *in vitro* evaluation of prototype six designed for case C and prototype seven designed for case D (Figure 5.6) are shown in Tables 5.3 and 5.4 respectively. In both prototypes the cutting guide was scored significantly better than the alignment guide. The seventh prototype was scored better than the sixth prototype.

The cutting guide of prototype six was scored good to excellent in every sub-category. The lower scores were mainly caused by the fitting of the guide base through the entire subtalar joint. Due to prohibited movement between talus and calcaneus in the 3D printed foot model, the cutting guide could not be fitted to the bone surface as planned. This caused instable fitting to the anatomy and a fixation k-wire without bone contact. Clearance of K-wire placement guidance was too big and has to be decreased for a stable fit.

The repositioning guide of prototype six was scored poor to excellent. The robustness, alignment rod and k-wire placement guidance were scored excellent, but the size, location, fitting, location of K-wires and general functionality were all scored poor. Guide seating was chosen on the cuboid and cuneiform bones, which are not visible during surgery and fitting was not unique. The number of K-wires the bare minimum and would ideally be increased.

The cutting guide of prototype seven was scored very good to excellent in all sub-categories. The alignment triangle was preferred over the alignment rod based on robustness, but the alignment K-wires should be placed further from the anatomy. Also, rounded corners of the cutting block were proposed for future PSGs.

The repositioning guide of prototype seven was scored fair to excellent. The location of this repositioning guide was better and more unique than that in prototype six, but was still not visible during surgery. The K-wires in the alignment triangle of the repositioning guide should also be placed further from the anatomy. The number of K-wires would ideally be increased to three and the location of the most superior K-wire should be changed to the location and orientation indicated in Figure 5.8.

Table 5.3: Evaluation by the orthopaedic surgeon of the sixth PSG prototype designed for case C

Category	Subcategories	Scores cutting guide					Scores repositioning guide				
		Poor	Fair	Good	Very good	Excellent	Poor	Fair	Good	Very good	Excellent
Design	- Size			X			X				
	- Robustness					X					X
	- Marks for placement	N/A					N/A				
	- Alignment rod					X					X
	- Cutting guidance block					X	N/A				
Fitting	- Location					X	X				
	- Unique fitting			X			X				
Fixation	- Number of K-wires					X			X		
	- Location of K-wires			X			X				
	- Orientation of K-wires					X				X	
	- K-wire placement guidance				X						X
Applicability	- General functionality				X		X				
	- Usability					X			X		

Table 5.4: Evaluation by the orthopaedic surgeon of the seventh PSG prototype designed for case D

Category	Subcategories	Scores cutting guide					Scores repositioning guide				
		Poor	Fair	Good	Very good	Excellent	Poor	Fair	Good	Very good	Excellent
Design	- Size					X			X		
	- Robustness					X					X
	- Marks for placement				X						X
	- Alignment triangle				X					X	
	- Cutting guidance block				X		N/A				
Fitting	- Location					X			X		
	- Unique fitting					X				X	
Fixation	- Number of K-wires					X				X	
	- Location of K-wires					X			X		
	- Orientation of K-wires					X					X
	- K-wire placement guidance					X					X
Applicability	- General functionality					X					X
	- Usability					X		X			

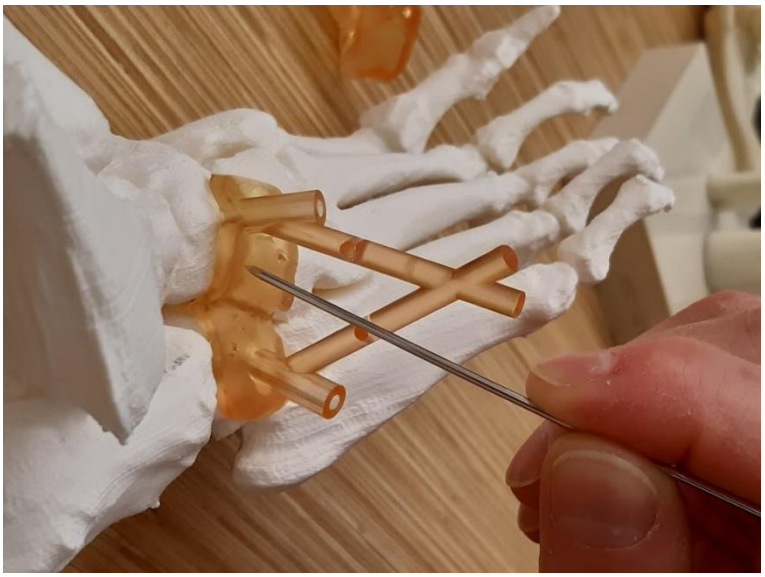

Figure 5.8: The 3D printed seventh prototype repositioning guide placed on the 3D printed foot of case D. The location and orientation of th eleft hollow cyclinder should be relocated to the location and orientation as indicated ny the orthopaedic surgeon.

Discussion

In this study, it was investigated how PSGs can be designed for application in complex foot surgery. For development of a PSG design protocol, one general PSG design was suggested for application in all cases of midfoot correction. In this process, seven prototypes were designed based on a list of prerequisites and virtual planning of three clinical cases of midfoot correction. Five general prototypes were designed for case B. Building on those designs, one prototype was designed for case C. Building on that design, one prototype was designed for case D. The final general design, which is included in the PSG design protocol consists of a proximal cutting/repositioning guide and a distal repositioning guide.

The common procedure for midfoot correction is a closing wedge osteotomy. Two osteotomies are planned, which define a wedge to be removed. The forefoot is rotated and translated to close the wedge and obtain a correct foot alignment. Earlier studies applying PSGs in complex foot surgery only developed cutting guides for correct execution of the planned osteotomies. (14,18,20) When only including cutting guidance in the PSG, repositioning of the forefoot remains dependant on the surgeon's experience and might result in a malalignment. In the prerequisites, it became apparent that repositioning guidance should be included in the PSG, as correct foot alignment plays an important role in lower limb function. Instead of designing separate cutting and repositioning guides, we combined both functionalities in one PSG. As the PSG combines both functionalities, removal of the cutting guide followed by placement of the repositioning guide is not necessary, which may result in a reduction in operating time.

During virtual planning, the second osteotomy plane would ideally be determined by execution of the initial osteotomy and repositioning of the forefoot. When designing a PSG for such a case, both the separate cutting and repositioning guides and the PSG with combined cutting and repositioning guide can be designed for intraoperative use. The use of separate cutting and repositioning guides has the advantage of a possible overlap in guide seating locations of the cutting guides as seen in the third general PSG prototype, as repositioning is executed using another PSG. This would allow for more cutting guidance options, such as k-wire guided cutting, a cutting slot and the cutting block used in all other PSG prototypes. In virtual planning of cases C and D, however, the second osteotomy plane could

not be determined preoperatively. Due to the cavus deformity, sufficient bone-to-bone contact could not be established when assuming complete rigidity of the foot. As opening of the joint capsule allows some flexibility, sufficient bone-to-bone contact could probably be established intraoperatively. Considering that this flexibility cannot be predicted, it cannot be accounted for during virtual planning and the second osteotomy has to be determined intraoperatively. When a second osteotomy cannot be determined preoperatively, the separate cutting and repositioning guides cannot be designed for intraoperative use, as executed osteotomies are required for placement of a repositioning guide. In such cases a PSG with combined cutting/repositioning guidance enables correct execution of the initial osteotomy and ensures correct alignment of the forefoot for intraoperative determination of the second osteotomy. Additionally, the second osteotomy can be guided visually by the cutting block designed for the initial osteotomy.

In this study, one general PSG design was proposed for application in all cases of midfoot correction of complex foot deformity. This design aids in the initial osteotomy and repositioning of the forefoot, as a second osteotomy plane cannot be determined in some cases of complex foot deformity. In some cases, however, it is possible to determine two osteotomy planes preoperatively. For these procedures, a PSG design containing cutting guidance for both osteotomies and repositioning guidance would be preferred over the current general PSG design. The general design of the fourth prototype, based on case B, could be used for design of this double cutting guide. Adaptation of this design might still be necessary, as it was not optimized in this study due to introduction of cases C and D.

In this study, the choice was made to design a combination of a proximal cutting/alignment guide and a distal alignment guide. This design would guarantee correct execution of the first osteotomy and aid in determination of the second osteotomy whilst allowing flexibility in the transverse arch after opening the joint capsule. When designing the alignment guide, however, the guide seating area spanned the entire height of the lateral side of the foot. This increases the chance of a unique and stable fitting, but inhibits all possible flexibility in the transverse arch. As flexibility in the transverse arch is required for correct intraoperative determination of the second osteotomy plane, the repositioning guide presented in this chapter needs further refinement. When redesigning the repositioning guide, both the guide seating location and size should be chosen differently to allow flexibility in the transverse arch during forefoot repositioning.

In conclusion, the cutting/repositioning guide of the seventh general PSG prototype fulfils the prerequisites sufficiently to for its fitting to be tested *in vivo.* The distal repositioning guide of the seventh general PSG prototype meets the surgeon's preferences, but the design must be adapted and evaluated for correct positioning and function *in vitro* before it can be tested *in vivo*.

Chapter 6 – General discussion

In this thesis, we studied how virtual planning and patient specific guides can be applied in and improve the outcome of complex foot surgery based on four patient cases. Workflows have been developed for obtaining virtual 3D foot models out of CT data, associated virtual planning of the surgical correction and PSG design for accurate translation of the virtual planning to the operating table. Additional reference documents have been created for correct execution of the developed workflows, such as an overview of the reference angles. The results reported in this thesis show the potential of application of 3D printed foot models and virtual planning in clinical practice. Further development and validation of PSGs is necessary before it can be applied in complex foot surgery.

As discussed in chapters three and four, assessment and correction of complex foot deformity is based on reference angles measured in lateral and DP 2D weightbearing radiographs. These reference angles describe the healthy alignment between two bones and are measured between reference lines indicating the longitudinal axis of the relevant bones. Preoperative assessment of the deformity is based on comparison of the measured reference angles to the normal values described in literature. The necessary corrections are planned by reconstructing the preoperatively measured reference angles into normal values. As virtual planning is executed using a 3D model constructed from supine CT data of the complex foot deformity, a translation from 2D reference angles to the 3D model is necessary for obtaining the most accurate result. In chapter three we studied how an accurate foot model can be acquired, which enables the use of the normal values of reference angles during the preoperative planning process of complex foot surgery. Using CT data of two patients, we developed a segmentation protocol for obtaining a 3D model and studied the difference between the natural supine alignment and the maximum achievable neutral alignment in rigid foot deformity. Based on the differences in measured reference angles between the supine and neutral foot alignment, we concluded that the foot should be positioned in a neutral alignment during CT acquisition. This ensures the optimal use of reference angles during virtual planning, which leads to the most accurate result. Additionally, the neutral foot alignment can be reproduced intraoperatively, thereby ensuring correct execution of planned osteotomies and the fit of a developed PSG. Based on these results, CT acquisition of complex foot deformity at MST is currently acquired from a neutrally aligned foot, as opposed to the supinely aligned foot in standard CT acquisition. This neutral alignment is achieved by manual redressing of the foot using a total contact cast.

Creation of virtual 3D foot models was executed via semi-automatic segmentation of CT data using functionalities in Materialise Mimics software. The initial foot model was extruded automatically via thresholding and region growing. Manual adaptation of this automatically extruded foot is needed, as osteopenia caused by limited weightbearing results in faded bone contours on CT images. Completing the faded bone contours is possible with a Materialise Mimics software functionality for automatic filling of gaps. However, when applying it in the complete foot model, it also fills up joint spaces. Application of this functionality to the complete foot model is therefore possible, but very time consuming due to manual correction of joint spaces and missed bone contours. Simplification of this process is possible by separation of the entire foot into separate bones using a Materialise Mimics software functionality. This enables automatic filling of each bone separately while avoiding closing of joint spaces, thereby limiting the time spent on manual editing. In this thesis, separation into all 28 bones was chosen, as this resulted in the most correct anatomical model and enabled clear visualization of all bones separately. The separation process, however, is also time consuming and may not be completely necessary as not all bones have to be visualized separately. In future, it might be possible to limit the separation into parts to the bones needed for measurement of reference angles and realignment during virtual planning. Another option for obtaining a complete anatomic 3D model

of the foot would be the development of an automatic segmentation method in another software package.

In chapter four we studied how virtual planning can be applied in and improve the outcome of complex foot surgery based on two patient cases. We developed a virtual planning protocol and compared foot anatomy between the preoperative foot, postoperative foot and planned result based on reference angles. These angles were measured in lateral and DP sketches containing projected outlines of relevant bones from CT data. In comparing retrospective planning to prospective planning, we found that the reference angles in the postoperative foot of the prospectively planned case were closer to the planned reference angle values and normal values than those measured in the retrospectively planned case. The results indicate that the application of virtual planning, even without the use of PSGs, improves the execution of the planned correction. As improvement of the correction has been indicated and there are no disadvantages to application of virtual planning in complex foot surgery, virtual planning can already be applied in future corrections. Considering that only two patients were studied, however, it is advisable to continue evaluating the postoperative outcome in future cases to validate the application of virtual planning in clinical practice.

In the current virtual planning protocol, the assumption is made that the foot is positioned in a neutral alignment. To achieve this alignment during CT acquisition, manual redressing is applied in complex foot deformities. However, seeing that redressing is a manual manipulation, it is a possibility that the resulting talocalcaneal alignment is not completely neutral. For correct translation of downward forces from the tibia through talus and calcaneus to the ground during the complete gait cycle, the talus and calcaneus should be aligned neutrally. Therefore, talocalcaneal alignment should be assessed preoperatively and corrected at the start of virtual planning if necessary to obtain the best postoperative result. This hindfoot correction can be achieved intraoperatively by opening the joint capsule and rotating the calcaneus to the correct alignment. This could be guided for instance by seating of a PSG on the realigned hindfoot and locking the alignment with osteosynthesis material. In future, the difference between virtual planning with and without hindfoot correction can be studied to determine whether this should be implemented in the virtual planning protocol.

Considering the non-weightbearing situation during surgery and the limited availability of weightbearing CT scanners, the 2D reference angles determined by Broos et al. (13) in non-weightbearing neutrally aligned feet were used as basis for virtual planning in chapter four. As reference angles are the basis of virtual planning, measurement and correction of these angles should be executed as accurate as possible. In this thesis, measurement of the reference angles was executed in 2D sketches containing the outline of relevant bones from CT data. This method was chosen, as it is a familiar representation for orthopaedic surgeons and uses the same data as used in virtual planning as opposed to radiographs. These sketches, however, do not contain density information about the bones in addition to these outlines. This additional information can increase the understanding of the bone anatomy and therefore improve the construction of the reference lines used in measurement of the reference angles. Three possible alternatives for measurement of reference angles using the same data as used in virtual planning are the construction of a Digitally Reconstructed Radiograph (DRR), determination of reference lines in the 3D space and complete measurement of reference angles in the 3D space. The use of a DRR was demonstrated by Broos er al. (13) for measurement of 2D reference angles. This has the same advantages as the use of a sketch with the additional benefit of density information. On the other hand, creation of a DRR is not possible in Materialise 3-Matic software used for virtual planning. Therefore, a translation from DRR to Materialise 3-Matic software and vice versa for measurement of reference angles during virtual planning is necessary. The second alternative is determination of the reference lines in the 3D space. Construction of reference lines can be executed

using the datum planes created for alignment during virtual planning. These datum planes indicate the longitudinal axis of the relevant bones in either DP or lateral view and are based on the 3D bone anatomy. The cross section of the DP and lateral planes is the reference line in the 3D space, which can be imported into the sketch for measurement of reference angles. The third alternative is complete measurement of the reference angles in the 3D space. This method uses the same reference lines as the second method. The reference angles are then measured in the 3D space, using the measuring tool of Materialise 3-Matic software. This tool can be used for measurement of 2D angles in the three orthogonal planes by ignoring the third dimension. This does require a correct anatomic orientation of the foot to ensure correct projection planes, but simplifies assessment of the foot deformity as creation of sketches is not necessary. In chapter four, measurement of reference angles was based on reference lines constructed in 2D sketches, as this was most like measurement in radiographs. The other methods, however, might result in more accurate or more reproducible measurements. Comparison of these four methods based on accuracy and inter- and intra-observer variability would be advisable to determine the method most suited for use in virtual planning of complex foot surgery.

In this thesis, we applied methods in virtual planning that are similar to the current preoperative planning process. Both measurement and correction of reference angles were based on and executed in 2D views of the 3D deformity. However, it is plausible that other methods based on and executed in the 3D space could improve the postoperative result even more. As mentioned by Broos et al. (13), 3D measurement of reference angles includes more information about the multiplanar deformity than the combination of lateral and DP 2D measurements, as it includes multiple degrees of freedom. Assessment of the deformity based on these 3D measurements in combination with the 2D measurements would provide the most complete set of information, as it combines the multiplanar nature of the deformity with the familiar reference angles. Before these 3D reference angles can be applied in assessment and virtual planning, a thorough understanding of these reference angles is needed. Therefore, it would be advisable to study the difference between 2D and 3D reference angles and how differences caused by deformities can be interpreted, to gain an understanding of their use and applicability in virtual planning.

In chapter five we studied how PSGs can be designed for application in complex foot surgery based on three cases of midfoot correction (cases B, C and D). PSG prototypes were developed based on a list of prerequisites and the virtual planning for the three cases. 3D printed prototypes were evaluated by one orthopaedic surgeon based on the design, fitting, fixation and expected functionality. Finally, a PSG protocol was developed describing the design of a general PSG for midfoot correction, which can be applied in and personalized for clinical cases. The functional requirements for the general PSG design were cutting guidance for planned osteotomies and bone repositioning guidance for obtaining the planned postoperative foot alignment. As mentioned by Popescu et al. (18) there are two options when designing both a cutting guide and a bone repositioning guide. Separate PSGs can be designed for both functionalities, or both functionalities can be combined in one PSG. We designed one PSG with both functionalities, as this fulfilled the functional requirements, is applicable in midfoot corrections and probably reduces manufacturing costs and operating time due to the single fitting. When planning cases C and D, sufficient bone-to-bone contact between hind- and forefoot could not be achieved with the assumption of rigidity. When accounting for flexibility in the transverse arch after opening of joint capsules, bone-to-bone contact could probably be sufficiently achieved intraoperatively. This flexibility, however, is unpredictable, causing an inability to define the distal osteotomy during virtual planning. As the proximal osteotomy and the alignment of the forefoot to the hindfoot can both be determined during virtual planning, we designed a PSG consisting of a proximal cutting/repositioning guide and a distal repositioning guide. These guides aid the surgeon in execution of the first osteotomy and repositioning of the forefoot, locking the forefoot in the planned

alignment. This alignment in combination with the initial cutting guidance aids the surgeon in intraoperative determination of the second osteotomy while allowing flexibility due to the opened joint capsule. Using the general PSG design developed in this thesis for midfoot correction, the second osteotomy has to be executed without a cutting guide. As the second osteotomy should be parallel to the first, the cutting guide of the first osteotomy can be used as reference for the orientation of the second osteotomy plane. Execution, however, is still dependent on the surgeon's experience. This can result in a differently oriented osteotomy plane than needed for obtaining the planned postoperative foot alignment, leading to possibly worse results or an increase in operating time due to the need for correction of the osteotomy. In further development of the current general PSG design for complex foot surgery, this dependency in execution of the second osteotomy would therefore ideally be prohibited. One solution might be creation of an adaptable cutting guide. This cutting guide would be locked in an orientation parallel to the proximal cutting guidance, but could be moved in distance to the determined position for the distal osteotomy. Further research is needed to determine how a cutting guide can be designed for execution of an intraoperatively determined the second osteotomy.

In conclusion, in this thesis it was described that virtual planning should be performed using a CT scan of a neutrally aligned foot. It was further shown that virtual planning may improve understanding of the necessary corrections preoperatively and intraoperatively and can improve the anatomic correction of bone malalignment as compared to the current treatment method. The addition of a PSG to the virtual planning can aid in accurate translation of the planned osteotomies to the operating table and may improve the postoperative result of complex foot surgery even further. Therefore, in this thesis it was shown that a PSG design consisting of a proximal cutting/repositioning guide and a distal repositioning guide is promising for midfoot correction for which a second osteotomy cannot be determined preoperatively. The design of the distal repositioning guide, however, must be improved in fitting, size and location and has to be evaluated *in vitro* and *in vivo* before it can be applied in complex foot surgery.

References

1. Moore KL, Dalley AF, Agur AMR. Clinically Oriented Anatomy. 7th ed. 2014. 522–658 p.
2. Agur AMR, Dalley AF. Grant's Atlas of Anatomy. 13th ed. 2013. 430–474 p.
3. Balasankar G, Ameersing L. Common Foot and Ankle Disorders in Adults and Children. Res J Text Appar. 2015;19(2):54–65.
4. Rosenbaum AJ, Lisella J, Patel N, Phillips N. The cavus foot. Med Clin North Am. 2014;98(2):301–12.
5. Raj MA, Tafti D, Kiel J. Pes Planus - StatPearls - NCBI Bookshelf [Internet]. August 3. 2021 [cited 2021 Sep 17]. Available from: https://www.ncbi.nlm.nih.gov/books/NBK430802/
6. Pinzur MS. Surgical treatment of the Charcot foot. Diabetes Metab Res Rev. 2016 Jan 1;32:287–91.
7. Lamm BM, Stasko PA, Gesheff MG, Bhave A. Normal Foot and Ankle Radiographic Angles, Measurements, and Reference Points. J Foot Ankle Surg [Internet]. 2016;55(5):991–8. Available from: http://dx.doi.org/10.1053/j.jfas.2016.05.005
8. Carrara C, Caravaggi P, Belvedere C, Leardini A. Radiographic angular measurements of the foot and ankle in weight-bearing: A literature review. Foot Ankle Surg. 2020 Jul 1;26(5):509–17.
9. Solomin LN, Ukhanov KA, Kirienko AP, Herzenberg JE. New Sagittal Plane Reference Parameters for Foot Deformity Correction Planning: The Vitruvian Foot. J Foot Ankle Surg. 2019 Sep 1;58(5):865–9.
10. Jansen RB, Svendsen OL. A review of bone metabolism and developments in medical treatment of the diabetic Charcot foot. J Diabetes Complications. 2018 Jul 1;32(7):708–12.
11. Doorgakant A, Davies MB. An Approach to Managing Midfoot Charcot Deformities. Foot Ankle Clin. 2020;25(2):319–35.
12. Sammarco VJ. Superconstructs in the Treatment of Charcot Foot Deformity: Plantar Plating, Locked Plating, and Axial Screw Fixation. Foot Ankle Clin. 2009 Sep;14(3):393–407.
13. Broos M, Berardo S, Dobbe JGG, Maas M, Streekstra GJ, Wellenberg RHH. Geometric 3D analyses of the foot and ankle using weight-bearing and non weight-bearing cone-beam CT images: The new standard? Eur J Radiol. 2021 May 1;138.
14. Dagneaux L, Canovas F. 3D Printed Patient-Specific Cutting Guide for Anterior Midfoot Tarsectomy. Foot Ankle Int. 2020 Feb 1;41(2):211–5.
15. Wirth SH, Espinosa N. The Use of Virtual Planning and Patient-specific Guides to Correct Complex Deformities of the Foot and Ankle. Foot Ankle Clin. 2020 Jun 1;25(2):257–68.
16. Kadakia RJ, Wixted CM, Allen NB, Hanselman AE, Adams SB. Clinical applications of custom 3D printed implants in complex lower extremity reconstruction. 3D Print Med. 2020 Dec;6(1).
17. Baraza N, Chapman C, Zakani S, Mulpuri K. 3D - Printed Patient Specific Instrumentation in Corrective Osteotomy of the Femur and Pelvis: A Review of the Literature. 3D Print Med. 2020 Dec;6(1).
18. Popescu D, Laptoiu D, Marinescu R, Botezatu I. Design and 3D printing customized guides for orthopaedic surgery – lessons learned. Rapid Prototyp J. 2018 Sep 20;24(5):901–13.

19. Popescu D, Laptoiu D. Rapid prototyping for patient-specific surgical orthopaedics guides: A systematic literature review. Proc Inst Mech Eng Part H J Eng Med. 2016 Jun 1;230(6):495–514.

20. Sobrón FB, Dos Santos-Vaquinhas A, Alonso B, Parra G, Pérez-Mañanes R, Vaquero J. Technique tip: 3D printing surgical guide for pes cavus midfoot osteotomy. Foot Ankle Surg. 2021;

21. Richter M, Seidl B, Zech S, Hahn S. PedCAT for 3D-imaging in standing position allows for more accurate bone position (angle) measurement than radiographs or CT. Foot Ankle Surg [Internet]. 2014;20(3):201–7. Available from: http://dx.doi.org/10.1016/j.fas.2014.04.004

22. Trepman E, Nihal A, Pinzur MS. Charcot Neuroarthropathy of the Foot and Ankle. Foot Ankle inter. 2005;26(1):46–63.

23. Rosenbaum AJ, DiPreta JA. Classifications in Brief: Eichenholtz Classification of Charcot Arthropathy. Clin Orthop Relat Res. 2015;473(3):1168–71.

24. Mulford JS, Babazadeh S, Mackay N. Three-dimensional printing in orthopaedic surgery: review of current and future applications. ANZ J Surg. 2016;86(9):648–53.

25. de Wouters S, Tran Duy K, Docquier PL. Patient-specific instruments for surgical resection of painful tarsal coalition in adolescents. Orthop Traumatol Surg Res [Internet]. 2014;100(4):423–7. Available from: http://dx.doi.org/10.1016/j.otsr.2014.02.009

26. Frykberg RG, Rogers LC. The Diabetic Charcot Foot: A Primer on Conservative and Surgical Management. J Diabet Foot Complicat. 2009;1(1):19–25.

27. Yang JCS, Chen CF, Luo CA, Chang MC, Lee OK, Huang Y, et al. Clinical Experience Using a 3D-Printed Patient-Specific Instrument for Medial Opening Wedge High Tibial Osteotomy. Biomed Res Int. 2018;2018.

28. Arunakul M, Amendola A, Gao Y, Goetz JE, Femino JE, Phisitkul P. Tripod index: a new radiographic parameter assesing foot alignment. Foot Ankle Int. 2013;34(10):1411–20.